Zoological Journal of the Linnean Society, 2008, **154**, 308–352. With 11 figures

Skull anatomy of the Oligocene toothed mysticete *Aetioceus weltoni* (Mammalia; Cetacea): implications for mysticete evolution and functional anatomy

THOMAS A. DEMÉRÉ[1]* and ANNALISA BERTA[2]

[1]*Department of Paleontology, San Diego Natural History Museum, PO Box 121390, San Diego, CA 92112, USA*
[2]*Department of Biology, San Diego State University, San Diego, CA 92182, USA*

Received 20 September 2007; accepted for publication 25 September 2007

Toothed mysticetes of the family Aetiocetidae from Oligocene rocks of the North Pacific play a key role in interpretations of cetacean evolution because they are transitional in grade between dorudontine archaeocetes and edentulous mysticetes. The holotype skull of *Aetiocetus weltoni* from the late Oligocene (28–24 Ma) of Oregon, USA, has been further prepared, revealing additional morphological features of the basicranium, rostrum and dentary that have important implications for mysticete evolution and functional anatomy. The palate of *Aetiocetus weltoni* preserves diminutive lateral palatal foramina and associated delicate sulci which appear to be homologous with the prominent palatal foramina and sulci that occur along the lateral portion of the palate in extant mysticetes. In modern baleen whales these foramina allow passage of branches of the superior alveolar artery, which supplies blood to the epithelia of the developing baleen racks. As homologous structures, the lateral palatal foramina of *A. weltoni* suggest that baleen was present in this Oligocene toothed mysticete. Cladistic analysis of 46 cranial and dental characters supports monophyly of the Aetiocetidae, with toothed mysticetes *Janjucetus* and *Mammalodon* positioned as successive sister taxa. *Morawanacetus* is the earliest diverging aetiocetid with *Chonecetus* as sister taxon to *Aetiocetus* species. *Zoological Journal of the Linnean Society*, 2008, **154**, 308–352.

ADDITIONAL KEYWORDS: palaeontology – phylogeny – systematics.

INTRODUCTION

Aetiocetidae (Cetacea, Mysticeti) comprises a relatively diverse family of archaic, small, toothed mysticetes found in Oligocene sedimentary rocks on both sides of the North Pacific (Barnes *et al.*, 1995). They represent an important transitional group that preserves morphologies intermediate between basilosaurid archaeocetes and edentulous mysticetes. The transitional status of aetiocetids should not be viewed as suggesting they were ancestral to all later diverging edentulous mysticetes, but instead that aetiocetids provide a glimpse of the morphological changes that occurred in early members of the mysticete clade as they evolved from bite-and-swallow predators to specialized bulk, filter-feeders.

To date, aetiocetids are only known from the North Pacific and can be considered an endemic lineage in that ocean basin until remains are discovered in other regions. The recent report of a new species of early Oligocene cetacean, *Willungacetus aldingensis*, from the Port Willunga Formation in South Australia (Pledge, 2005) provisionally assigns this southern hemisphere taxon to the Aetiocetidae. This record, however, still needs to be confirmed. Two of the four nominal aetiocetid genera are monotypic, *Ashorocetus* and *Morawanocetus*, both from the Morawan Formation near Ashoro, Hokkaido, Japan (Barnes *et al.*, 1995). *Chonecetus* includes two species, *C. sookensis* (Russell, 1968) from the Hesquiat Formation on

*Corresponding author. E-mail: tdemere@sdnhm.org

Vancouver Island, British Columbia, Canada, and *C. goedertorum* (Barnes & Furusawa in Barnes *et al.*, 1995) from the Pysht Formation, Olympic Peninsula, Washington, USA. *Aetiocetus*, the most speciose genus, is represented by *A. cotylalveus* Emlong, 1966 and *A. weltoni* Barnes & Kimura in Barnes *et al.*, 1995, both from the Yaquina Formation of coastal Oregon, USA, and *A. tomitai* Barnes & Kimura in Barnes *et al.*, 1995 and *A. polydentatus* Sawamura in Barnes *et al.*, 1995 from the Morawan Formation near Ashoro, Hokkaido, Japan. The assignment of *A. polydentatus* to the genus *Aetiocetus* has been recently questioned (Ichishima, 2005; Fitzgerald, 2006), a conclusion with which we disagree. Additional undescribed aetiocetids are reported from the upper Oligocene San Gregorio Formation near La Paz, Baja California Sur, Mexico (Gerardo-Gonzalez-Barba, pers. comm. cited in Barnes *et al.*, 1995).

The presence of teeth and primitive cranial and rostral features led to initial consideration of *Aetiocetus cotylalveus* as an archaeocete (Emlong, 1966), although its many mysticete features were emphasized in that report. Later, Van Valen (1968) assigned *A. cotylalveus* to the Mysticeti, noting that the ancestors of mysticetes must have had teeth and that *Aetiocetus* in other respects was more similar to mysticetes than to archaeocetes. Although differing on higher-level relationships, both Emlong and Van Valen recognized the phylogenetically basal nature of *Aetiocetus cotylalveus* and its importance as a transitional cetacean taxon.

Since the 1960s a number of additional toothed mysticete fossils have been discovered and described and the definition of the family Aetiocetidae as originally proposed by Emlong (1966) has been modified to include up to eight species in possibly four genera (Barnes *et al.*, 1995). These authors proposed a phylogenetic hypothesis for the Aetiocetidae and named three subfamilies to contain this expanded diversity: Chonecetinae (*Chonecetus* spp.), Morawanocetinae (*Morawanocetus yabukii*) and Aetiocetinae (*Ashorocetus eguchii* and *Aetiocetus* spp.). In a later report, Sanders & Barnes (2002) established the superfamily Aetiocetoidea to include all then known toothed mysticetes: Aetiocetidae (Emlong, 1966), Llanocetidae (Mitchell, 1989), and Mammalodontidae (Mitchell, 1989). As recently shown by Fitzgerald (2006), however, there is ample evidence that Aetiocetoidea is a grade taxon and that the many described species, genera and families of toothed mysticetes do not represent a monophyletic group. For example, possession of teeth is clearly a primitive condition and among toothed mysticetes there is considerable morphological variation in tooth shape, size, position and number. The recent mysticete phylogeny proposed by Fitzgerald (2006) recognizes six toothed lineages: (1) ChMTM (an undescribed purported toothed mysticete from the Oligocene of South Carolina, USA; Geisler & Sanders, 2003); (2) Llanocetidae (a large toothed mysticete from the latest Eocene or earliest Oligocene of the Antarctic Peninsula, *Llanocetus denticrenatus* was not included in Fitzgerald's phylogenetic analysis but was mentioned in the text); (3) Janjucetidae (a short-faced toothed mysticete from the late Oligocene of Victoria, Australia); (4) Mammalodontidae (a small-headed toothed mysticete from the late Oligocene of Victoria, Australia); (5) a paraphyletic Aetiocetidae represented by a *Chonecetus* clade (only *C. goedertorum* was considered); and (6) an *Aetiocetus* clade (only *A. cotylalveus* was considered). Although not included in the actual cladistic analysis, *A. polydentatus* is considered by Fitzgerald (2006) not to be a member of *Aetiocetus* because of possession of several purported derived features: (1) ascending process of maxilla terminating slightly posterior to antorbital notch, at a point level with the anterior third (anteroposteriorly) of the supraorbital process of frontal; (2) anteroposteriorly foreshortened supraorbital process of frontal; (3) concavity in lateral margin of supraorbital process poorly developed with orbit opening laterally but not anterolaterally and dorsolaterally as in more basal mysticetes; and (4) elongated intertemporal region with well-developed sagittal crest.

The controversial monophyly, definition and membership of Aetiocetidae is not just a semantic nomenclatural debate. Instead, it underlines the importance of this taxon in the interpretation of basal mysticete phylogenetic relationships and functional hypotheses of character evolution related to the loss of an adult dentition and development of a palatal baleen filter. One of the obstacles to resolving the issue of aetiocetid monophyly is the current paucity of detailed morphological descriptions and illustrations of nominal taxa. The present report attempts partially to rectify this problem by presenting a thorough redescription of the holotype skull and dentary of one of the better-preserved aetiocetids, *Aetiocetus weltoni*. Insights gained through this analysis of key morphological features and their taxonomic distribution among stem mysticetes is then used to re-evaluate phylogenetic relationships of nominal aetiocetids.

MATERIAL AND METHODS

Measurements, to the nearest tenth of a millimetre, of crania, dentitions and dentaries were taken using digital and/or mechanical calipers; these measurements are provided in Tables 1–4.

The following aetiocetid fossils were studied for this report: (1) USNM 25210, holotype skull of *Aetiocetus cotylalveus* Emlong, 1966; (2) USNM 256593, partial skeleton of undescribed specimen here referred to

Table 1. Measurements (cm) of the skull of *Aetiocetus weltoni* UCMP 12290 and *Aetiocetus cotylalveus* USNM 25210

Measurement	UCMP 12290	USNM 25210
Condylobasal length	61.6	62.3
Rostral length (functional)	33.0	34.0
Braincase length (functional)	28.6	28.3
Rostral width (infraorbital plate)	20.9	20.8
Rostral width 2 (25%)	16.8	16.3
Rostral width 3 (50%)	13.6	12.6
Rostral width 4 (75%)	9.0	7.3
Rostral width 5 (pmx/max suture)	6.8	6.4
Premaxilla width 1 (25%)	15.0	2.3
Premaxilla width 2 (50%)	2.4	3.0
Premaxilla width 3 (75%)	2.8	2.7
Nasal length (greatest)	13.8	11.8
Nasal width (anterior width)	5.0e	3.7
Maxilla width 1 (antorbital notch)	7.3	7.1
Maxilla width 2 (25%)	5.7	4.9
Maxilla width 3 (75%)	1.4	2.7
Ascending process max. (width)	3.7	3.8
Ascending process max. (length)	7.8	6.6
Supraorbital process max. W (medial)	–	11.1
Suprorbital process max. W (lateral)	8.2	8.3
Occipital shield width	24.1	25.2
Occipital shield height	–	10.0
Occipital condyle width	9.7	9.0
Occipital condyle height	6.1	5.7
Zygomatic width	28.7	31.6
Palate length (straight line)	45.4	52.8
Palate length (curve)	46.1	–
Palate chord	2.5	–
Palatine length	11.8	15.5e

e, estimated measurement.

A. cotylalveus; (3) AMP 2, holotype cranium of *Aetiocetus tomitai* Kimura & Barnes in Barnes *et al.*, 1995; (4) AMP 12, holotype skeleton of *Aetiocetus polydentatus* Sawamura in Barnes *et al.*, 1995; (5) NMC 6443, holotype cranium of *Chonecetus sookensis* Russell, 1968; (6) LACM 131146, holotype cranium of *Chonecetus goedertorum* Barnes & Furusawa in Barnes *et al.*, 1995; (7) LACM 138027, paratype partial cranium and dentary of *C. goedertorum*; and (8) AMP 1, holotype partial skull and dentition of *Morawanocetus yabukii* Kimura & Barnes in Barnes *et al.*, 1995. The following specimens and/or published literature were used for outgroup comparison: (1) *Tasmacetus shepardi* (USNM 484878); (2) *Agorophius* sp. (ChM PV5852); (3) *Agorophius pygmaeus* (MCZ 8761; discussed in Fordyce, 1981); (4) *Dorudon atrox* (numerous specimens discussed in Uhen, 2004); and (5) *Zygorhiza kochii* (USNM 11962). The following specimens were used for ingroup comparison: (1) *Mammalodon colliveri* (cast of NMV P199986); (2) *Janjucetus hunderi* (published description and illustrations of NMV P216929); (3) *Eomysticetus whitmorei* (ChM PV4253); and (4) representative taxa of modern mysticetes (see Deméré, Berta & McGowen, 2005).

Acronyms for institutions housing specimens discussed in this study are as follows: AMP, Ashoro Museum of Paleontology, Ashoro, Hokkaido, Japan; ChM, Charleston Museum of Natural History, Charleston, South Carolina, USA; LACM, Natural History Museum of Los Angeles County, Los Angeles, California, USA; MCZ, Museum of Comparative Zoology, Harvard University, Boston, Massachusetts, USA; NMC, National Museum of Canada, Ottawa, Canada; NMV, National Museum of Victoria, Melbourne, Australia; UCMP, Museum of Paleontology, University of California, Berkeley, California, USA; UO, Museum of Natural History, University of Oregon, Eugene, Oregon, USA; USNM, National Museum of Natural History, Smithsonian Institution, Washington, DC, USA.

The holotype skull and dentary of *Aetiocetus weltoni* was examined using computed tomography

Table 2. A, measurements (cm) of the left dentary of *Aetiocetus weltoni* UCMP 122900; B, measurements (mm) of cross-sectional dimensions measured at various points along the left dentary

(A)	
Total length (straight line)	54.5
Total length (outside curvature)	55.2
Length of chord	1.8e
Number of mental foramina	7.0
Condyle to coronoid process	6.3
Coronoid crest length	17e
Condyle to mandibular foramen	7.7
Minimum height neck	8.2
Mandibular condyle vertical diameter	5.3
Mandibular condyle transverse diameter	3.5
Mandibular foramen height	7.7e
Mandibular foramen width	2.5e
Mandibular symphysis length	3.2
Symphyseal groove length	4.5
(B)	
Vertical/transverse diameter @ 12.5% of dentary total length	43.3/19.4
Vertical/transverse diameter @ 25% of dentary total length	38.5/21.1
Vertical/transverse diameter @ 37.5% of dentary total length	37.1/23.3
Vertical/transverse diameter @ 50% of dentary total length	42.1/22.4
Vertical/transverse diameter @ 62.5% of dentary total length	52.0/22.3
Vertical/transverse diameter @ 75% of dentary total length	85.2/27.2
Vertical/transverse diameter @ coronoid process	161.4/31.7
Vertical/transverse diameter @ posterior end	86.7/52.4

e, estimated measurement.

Table 3. Measurements (mm) of upper dentition of *Aetiocetus weltoni* UCMP 122900

Distance from anterior terminus of maxilla to centre of tooth alveolus	
I1	2.0
I2	4.5
I3	8.0
C	11.2
P1	14.2
P2	17.7
P3	21.0
P4	24.5
M1	27.9
M2	30.8
M3	33.2
I1, AP/T	6.3/4.9
I2, AP/T	7.8/5.2/11.9
I3, AP/T/H	8.8/5.8/11.0
C, AP/T/H	8.3/4.9/11.4
P1, AP/T	8.9/5.4/10.4
P2, AP/T/H	10.6/6.2/12.2
P3, AP/T	10.6/6.5d/9.6
M2, AP/T	11.1/7.2/10.0e
M3, AP/T	10.7/5.7/10.3e

AP, anteroposterior; d, distorted; e, estimated measurement; H, crown height, T, transverse.

(CT) techniques. The resulting scan images are stored in the Department of Paleontology, San Diego Natural History Museum.

LOCATION, STRATIGRAPHY AND CORRELATION

The holotype of *Aetiocetus cotylalveus* was collected from the Yaquina Formation as exposed intertidally on the modern marine abrasion platform near the mouth of Deer Creek between Seal Rock State Park and the mouth of Beaver Creek, Lincoln County, Oregon, USA (UO Locality 2503). As reported by Emlong (1966) and Snaveley *et al.* (1976), the Yaquina Formation here consists of a north-west-dipping (19°) sequence of interbedded, grey, fine-grained sandstones, medium-grained sandstones, and siltstones containing fossils of marine molluscs, as well as carbonized wood. Emlong (1966: fig. 1) considered UO Locality 2503 to occur stratigraphically high in the Yaquina Formation, not far below its depositional contact with the overlying Nye Mudstone. In fact, Emlong noted that the contact between the two rock units 'is visible west of the type locality at times of extreme minus tide, but is normally below sea level.' The type locality of *Aetiocetus weltoni* (UCMP locality V-79013) occurs less than 1 km north of UO Locality 2503 in the Yaquina Formation as also exposed intertidally on the modern abrasion platform at Ona Beach near the mouth of Beaver Creek, Lincoln County, Oregon, USA. Although Barnes *et al.* (1995) asserted that UCMP Locality V-79013 is stratigraphically higher in the Yaquina Formation than UO Locality 2503, given the general north-east strike (N20°E) of the strata at each locality, both sites may represent the same general stratigraphic horizon in the uppermost portion of this rock unit. Without more detailed fieldwork it is not certain how much, if any, stratigraphic thickness (and therefore time) separates the two fossil localities.

The Yaquina Formation was originally named by Harrison & Eaton (1920) for shallow-water marine deposits exposed in the vicinity of the village of Yaquina, near Newport, Oregon. Addicott (1976) correlated the Yaquina Formation in the Newport

Table 4. Measurements (mm) of lower dentition of *Aetiocetus weltoni* UCMP 122900

Distance from anterior terminus of mandible to centre of tooth alveolus	
i1	8
i2	25
i3	57
c	95
p1	127
p2	159
p3	200
p4	234
m1	264
m2	292
m3	325e
m4	340
i1, AP/T	6.7/6.4
i2, AP/T	8.3/6.9
i3, AP/T/H	8.8/7.4/11.4
c, AP/T/H	–/–/11.3
p1, AP/T	10.1/7.1
p2, AP/T/H	–/–/14.6
p3, AP/T	8.2/5.1
p4, AP/T	10.5/6.9
m1, AP/T	–/6.4
m2, AP/T	–/6.4
m3, AP/T	11.1/4.9
m4, AP/T	8a/–

a, alveolus; AP, anteroposterior; e, estimated measurement; H, crown height; T, transverse.

Embayment with his Juanian provincial molluscan stage and with the Vaqueros provincial molluscan stage of California. Rau (1981) reported benthic foraminifers from the Yaquina Formation that were correlative with the Zemorrian provincial benthic foraminifer stage of Kleinpell (1938). Armentrout (1981) citing C. A. Repenning (pers. comm.) reported the co-occurrence of Zemorrian benthic foraminifers, Juanian marine molluscs and Arikareean marine mammals in the Yaquina Formation as exposed in the Yaquina Bay section near Newport. These various biochronological correlations led Armentrout (1981) to suggest a late late Oligocene (late Chattian) age for the Yaquina Formation (approximately 24–25 Ma). In a more recent palaeomagnetic analysis of Pacific Coast Palaeogene chronostratigraphy, Prothero *et al.* (2001) sampled the Yaquina Formation and correlated the uppermost portion of the rock unit with Chron C9r, suggesting an older age for this stratigraphic interval of 28 Ma, early late Oligocene (early Chattian). Based on this correlation web the late Oligocene age of the holotype of *A. weltoni* is confirmed. However, its absolute age may be older than previously thought, perhaps as old as early late Oligocene (approximately 28 Ma).

SYSTEMATICS

Order Cetacea

Suborder Mysticeti

Family Aetiocetidae Emlong, 1966

Genus Aetiocetus Emlong, 1966

Type species: Aetiocetus cotylalveus Emlong, 1966

Distribution: Late Oligocene of Oregon and Japan

Included species: Aetiocetus cotylalveus Emlong, 1966, *A. polydentatus* Sawamura in Barnes *et al.*, 1995, *A. tomitai* Kimura & Barnes in Barnes *et al.*, 1995, *A. weltoni* Barnes & Kimura in Barnes *et al.*, 1995.

Definition: The monophyletic group containing the most recent common ancestor of *Aetiocetus cotylalveus* and *A. polydentatus* and all of its descendants.

Emended diagnosis: Small toothed mysticetes with three or fewer small and simple anterior and posterior denticles on posterior upper teeth, anterior and postcanine teeth weakly heterodont (synapomorphies of species of *Aetiocetus*); triangular anterior extension of parietal–frontal suture, fine vertical enamel ridges only on lingual surface of postcanine teeth, wide diastemata between postcanine teeth, and rostral width at antorbital notch relative to occipital condyle width > 170% (possible synapomorphies of species of *Aetiocetus*); lacrimal with large and lobate dorsal exposure, palate window exposing vomer present and formed by maxilla and premaxilla, and distinct internal narial notch formed by palatine, pterygoid and vomer (synapomorphies of *Aetiocetus* + *Chonecetus*); zygomatic process of squamosal expanded near its anterior margin and at its posterior end but narrow in its middle, short overlap of jugal by squamosal, and coronoid process of dentary well developed with concave posterior margin (aetiocetid synapomorphies); mandibular symphysis not sutured, descending process of maxilla developed as an edentulous infraorbital plate, anterior and postcanine teeth moderately to weakly heterodont or absent (apomorphies shared with toothed and edentulous mysticetes); supraorbital processes of frontal elevated and at same level as cranial vertex, distinct intertemporal region, anteriorly placed external narial opening, and retention of adult dentition (plesiomorphies shared with dorudontine archaeocetes).

AETIOCETUS WELTONI BARNES & KIMURA IN BARNES *ET AL.*, 1995

AETIOCETUS SP. NOV. KIMURA, BARNES & FURUSAWA, 1992

AETIOCETUS WELTONI BARNES & KIMURA, IN BARNES *ET AL.*, 1995

Emended diagnosis: A species of *Aetiocetus* with deeply concave orbital rim of supraorbital process of frontal and posteriormost edge of ascending process of maxilla terminating at posterior border of supraorbital process of frontal (autapomorphies of *A. weltoni*); narrower transverse intertemporal width, more robust zygomatic process of the squamosal, and less lobate anterior parietal wings (symplesiomorphies relative to *A. cotylalveus*); non-polydont upper dentition, minor overhang of temporal wall by lambdoidal crests, and narrower nasals (symplesiomorphies relative to *A. polydentatus*).

Holotype: UCMP 122900, including associated elements of one individual consisting of a nearly complete skull (missing most of the supraoccipital), right and left dentaries, partial hyoid skeleton, cervical, thoracic, lumbar and caudal vertebrae, and some ribs. Only the skull and dentaries have been prepared to date.

Locality: UCMP Locality V-79013, Ona Beach, Lincoln County, Oregon, USA.

Stratigraphic horizon and age: Yaquina Formation (upper part); late Oligocene, Chattian, ~24–28 Ma.

DESCRIPTION

GENERAL FEATURES OF SKULL

The holotype skull of *Aetiocetus weltoni* (UCMP 122900) is nearly complete, lacking the right exoccipital (reconstructed with an epoxy prosthesis), the anterior 60% of the supraoccipital shield and the dorsalmost portions of the parietals at the anteromedial corner of the temporal fossa. Although both tympanic bullae were found *in situ*, breakage through the basicranium (which probably occurred at the time of recovery) has resulted in damage to both petrosals. The right exoccipital is also missing. The right and left dentaries were articulated with the rostrum at the time of burial and through sediment compaction and diagenesis became solidly attached to the alveolar margin of the upper jaw. Because of this, upper and lower teeth are in a forced 'clenched' position and a few teeth in each tooth row have been driven into the over- or underlying bones (i.e. lower teeth forced into the palatal surface of the maxilla and the upper teeth forced into the alveolar margin of the dentary). Subsequent mechanical preparation work has removed the entire left dentary and the posterior half of the right dentary from the skull. The degree of closure of cranial sutures (closed, but not fused) suggests that the skull belonged to a subadult individual.

The functional rostrum (tip of rostrum to antorbital notch) forms 54% of the condylobasal length (CBL) and is broadly triangular in dorsal aspect (Table 1). The external narial fossa is anteriorly placed well in front of the antorbital notch, and its posterior border (defined by the anterior margin of the nasals) lies at a level midway between the midpoint of the rostrum and the back of the nasal bones. The ascending process of the maxilla and premaxilla extend posteromedially across the anteromedial corner of the frontal to the level of the root of the postorbital process of the frontal (Figs 1, 2). The functional cranium (antorbital notch to occipital condyles) forms 46% of CBL (Table 1). The supraorbital processes of the frontals are elevated and lie at the same level as the cranial vertex (Fig. 1). The temporal fossae are large and ovate and the intertemporal constriction is relatively long and narrow. The zygomatic process of the squamosal reaches anteriorly to contact the postorbital process of the frontal (Fig. 3). The dentition retains a minor degree of heterodonty and has a tooth count of 11/12. Upper and lower teeth occlude in an alternating, interlocking pattern (Fig. 4). The dentary has a large mandibular foramen and a lobate coronoid process positioned within the temporal fossa. The symphysis is unfused with a distinct symphyseal groove.

PREMAXILLA

On the dorsal surface of the rostrum the right and left premaxillae are unfused but closely appressed at the midline between the tip of the rostrum and the level of I3. Posterior to I3 the medial borders of the premaxillae diverge from one another to expose the mesorostral groove (Fig. 2). This condition occurs in all species of *Aetiocetus* and is not unlike the condition in later diverging edentulous mysticetes. The anterior terminations of the premaxillae are narrowly triangular in dorsal aspect and form a low crest where they meet at the midline. At the level of the canine on the left side and the I3-C diastema on the right side is a single anterior premaxillary foramen opening anteriorly and positioned within 10 mm of the maxilla–premaxilla suture. A second foramen occurs on the right side at the level of the I2-3 diastema. There is no foramen in this position on the left side. These appear to be the only foramina on the premaxilla. There are no premaxillary foramina in the area adjacent to the narial fossa, nor are there

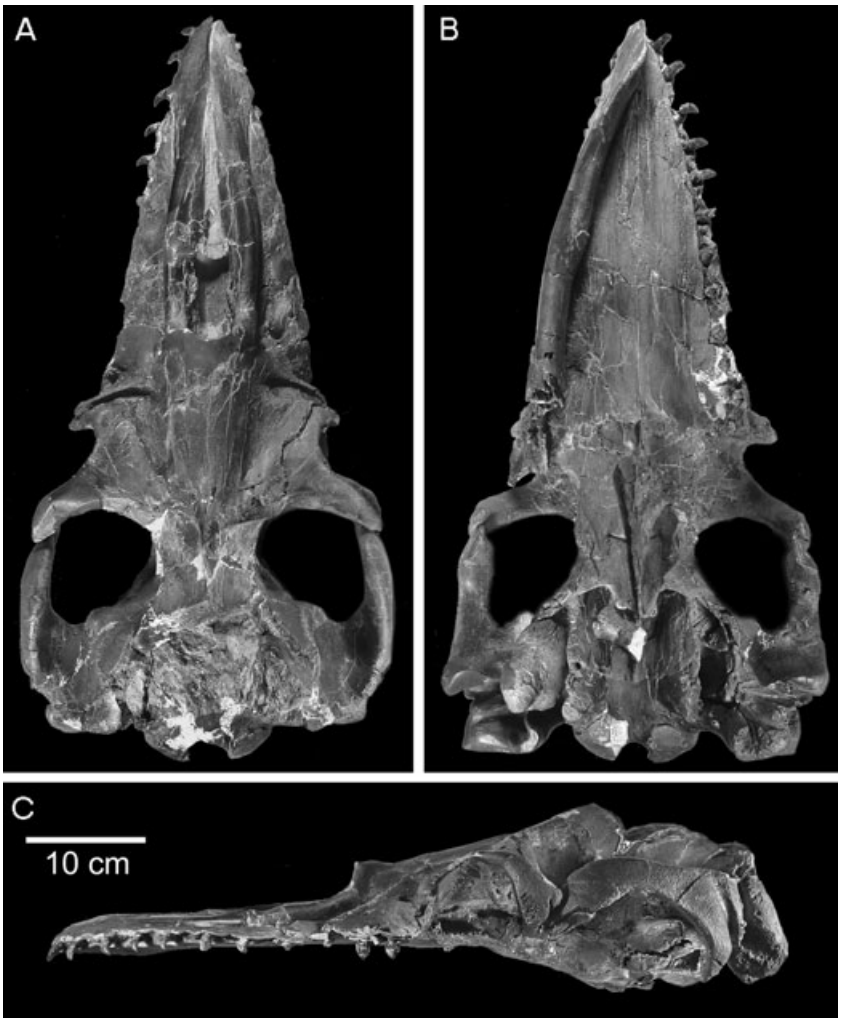

Figure 1. *Aetiocetus weltoni*, UCMP 122900, holotype skull. A, dorsal view; B, ventral view; C, left lateral view.

any sulci (anteromedial, posteromedial, or posterolateral sulci) as occur in stem and crown odontocetes. Posterior to the canine the dorsal surface of the premaxilla becomes distinctly elevated above the surface of the adjacent maxilla. Although the two bones are closely appressed, the intervening suture appears to have been unfused, a condition possibly associated with rostral kinesis in later diverging mysticetes. The condition in archaeocetes (e.g. *Zygorhiza*) has the premaxillae fused anteriorly at the level of I1 and unfused posteriorly at the level of I3. In *Janjucetus* and *Mammalodon* the condition at the tips of the premaxillae appears to be equivocal due to poor preservation. However, in *Janjucetus* it is clear that the premaxilla in this region is more elevated above the adjacent maxilla than in species of *Aetiocetus*. In *A. weltoni* the elevation of the premaxilla increases posteriorly and is most pronounced along the lateral half of the premaxilla, especially between P1 and M2. In this region the lateral surface of the premaxilla is broadly rounded and overhangs the medial margin of the adjacent maxilla. Medially, the surface of the premaxilla in this region slopes inward toward the mesorostral groove. The resulting embayment represents the anterior portion of the external narial fossa. At about the level of P4 (roughly corresponding to the middle of the narial fossa) the premaxilla narrows abruptly as its medial margin becomes more steeply sloped. At the level of M1 (roughly corresponding to the posterior part of the narial fossa) the lateral portion of the premaxilla ascends steeply to meet the adjacent nasal bone. The anterolateral corner of the nasal–premaxilla suture is marked by a rugose process (the 'crest-like eminence' of Barnes *et al.*, 1995) that is divided by this suture. Posterior to this region the premaxilla gradually ascends across the frontal to the cranial vertex and is in tight sutural contact with the nasal and maxilla until their mutual

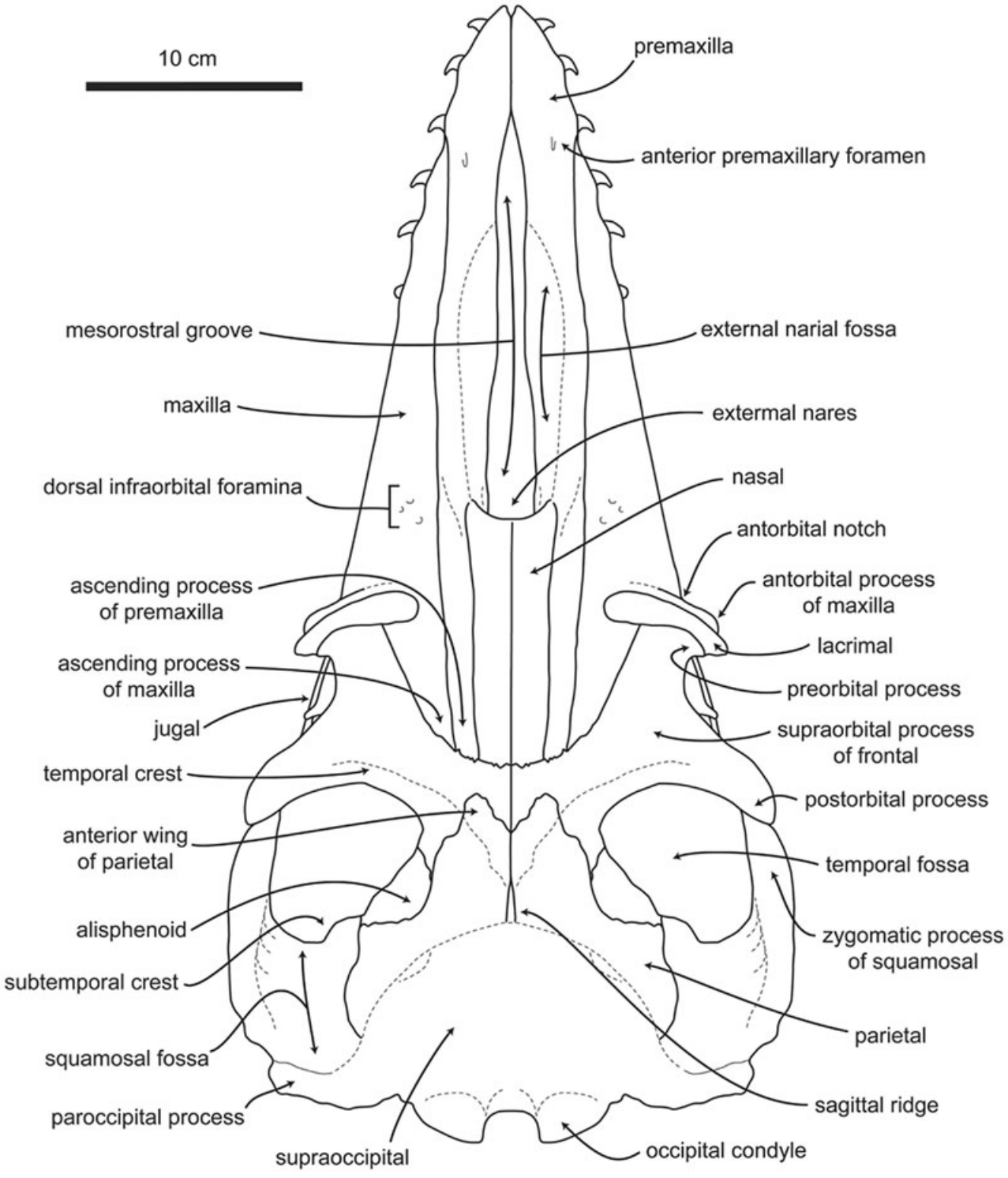

Figure 2. *Aetiocetus weltoni*, reconstructed skull in dorsal view showing anatomical features.

posterior terminations. The sutures between the nasal, premaxilla and maxilla in this region appear to be fused, suggesting a lack of kinesis in the posterior portion of the rostrum. The ascending process of the premaxilla is fairly uniform in transverse width and measures approximately 13–14 mm in that dimension. The posterior termination of the premaxilla occurs slightly (approximately 8 mm) in front of the

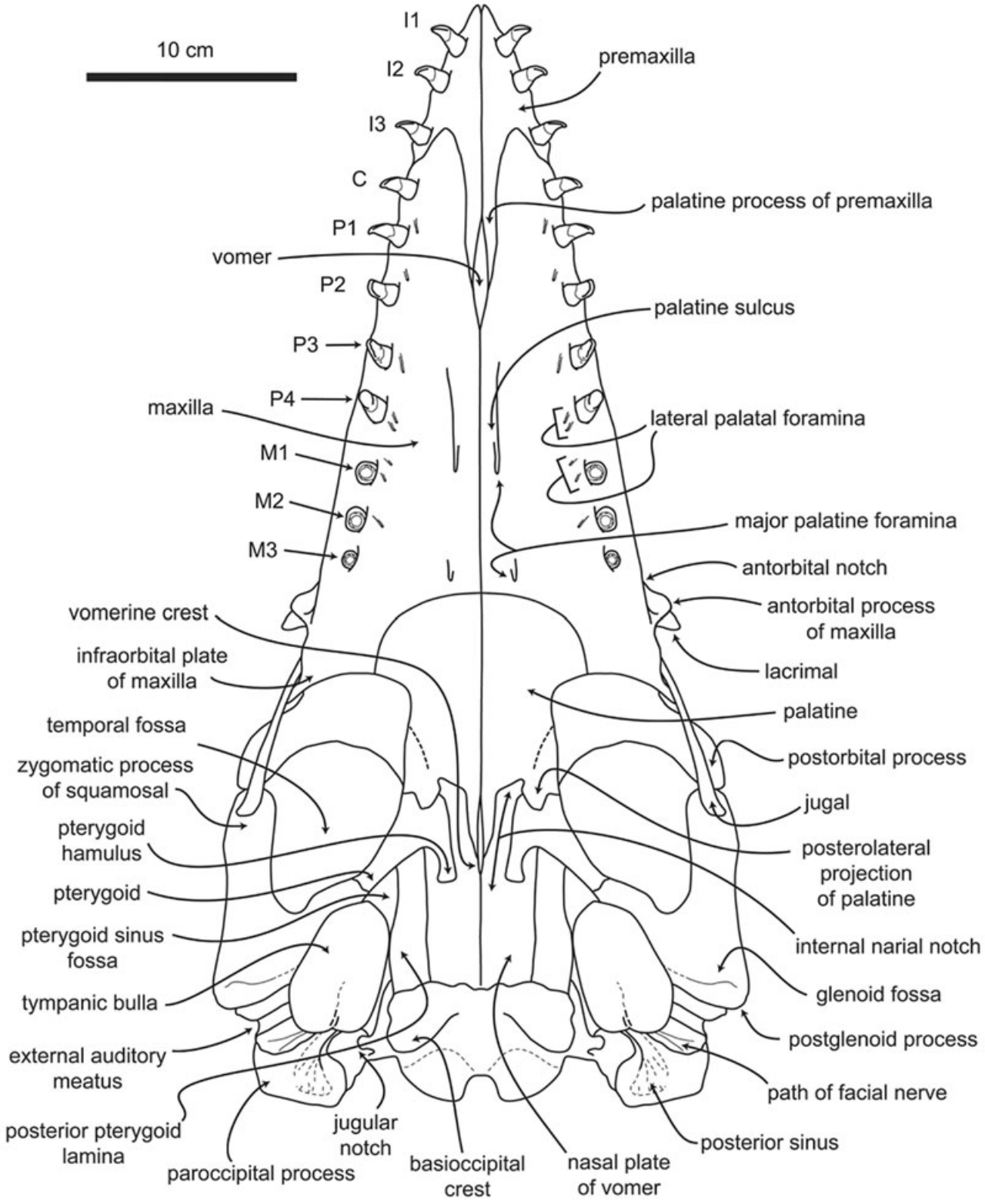

Figure 3. *Aetiocetus weltoni*, reconstructed skull in ventral view showing anatomical features.

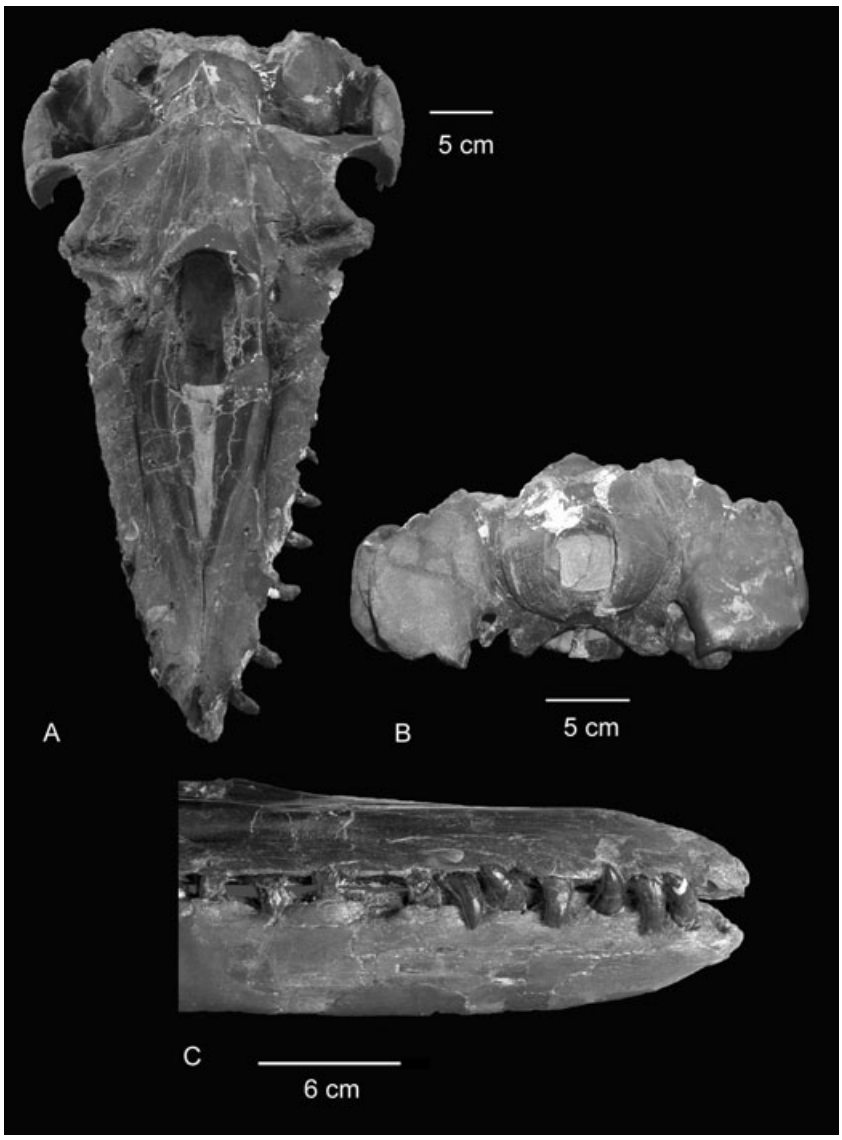

Figure 4. *Aetiocetus weltoni*, UCMP 122900, holotype skull. A, anterodorsal view; B, posterior view; C, lateral view of right anterior upper and lower dentition.

termination of the nasals, which occurs at the level of the temporal crest on the posterior portion of the postorbital process of the frontal. In *Aetiocetus cotylalveus* (USNM 25210), *Chonecetus goedertorum* (LACM 131146) and *Janjucetus hunderi* (NMV P216929) the rostral telescoping is less pronounced and the nasal terminates more anteriorly and at the level of the middle of the orbit. The condition in *Aetiocetus polydentatus* (AMP 12) is like that in *A. weltoni*. In *Janjucetus* the premaxilla does not overhang the maxilla, tapers sharply between the nasal and the maxilla, and terminates posteriorly in front of the posterior terminations of both elements at the level of the preorbital process of the frontal.

On the palate, the premaxillae are only exposed at the anterior end of the rostrum where they meet at the midline. Posteriorly the premaxilla forms a complex suture with the maxilla and vomer (Figs 1B, 3). The latter is exposed in a narrow palatal window formed posteriorly by the maxillae and anteriorly by the palatine processes of the premaxillae. Medially, the palatine processes of the premaxillae have a narrow exposure between the anterior tips of the maxillae, while posteriorly they bifurcate and surround the anterior half of the narrow vomer exposure. The posterior terminations of the palatine processes extend to the level of P2. Anteriorly, the right and left portions of the premaxilla meet at the midline at the

level of the anterior border of Pl (at the middle of C in *A. cotylalveus*). The intra-premaxillary suture at the midline is open and unfused from the vomer exposure to the tip of the rostrum. Laterally, the premaxilla contacts the maxilla along a posterolaterally directed suture. This suture, although tight, appears to have also been unfused based on the presence of a 1-mm-thick seam of siltstone matrix between the two bones. Anteriorly, this suture is orientated in the parasagittal plane beginning at the level of P2 and extending to the level of I3 at which point the suture turns laterally then posterolaterally as it ascends through the middle of the I3-C diastema to emerge on the dorsal surface of the rostrum. Within the diastema a distinct embrasure pit for the lower canine occurs on the anterior margin of the suture.

Maxilla

On the dorsal surface of the rostrum the maxilla forms an open suture with the adjacent premaxilla as previously described. The contact, however, between the maxilla and the premaxilla is a tight articulation as in archaeocetes and unlike the much looser, kinetic condition in modern mysticetes. Posteriorly the suture is recessed adjacent to the level of the external nares (narial fossa) and is obscured from dorsal view by the overhanging lateral wall of the premaxilla. An acutely triangular ascending process of the maxilla extends onto the anteromedial portion of the frontal remaining in tight sutural contact with the ascending process of the premaxilla. Both processes appear to be firmly sutured into the frontal unlike the relatively loose articulation seen in later diverging mysticetes (e.g. *Balaenoptera* spp.). On the rostrum the thin lateral margin of the maxilla is slightly scalloped corresponding to the interlocking occlusion of the upper and lower dentition. Embayed regions of the lateral margin correspond to placement of crowns of the lower teeth, while convex regions correspond to the position of roots of the upper teeth. In the holotypes of *A. cotylalveus* (USNM 25210) and *A. polydentatus* (AMP 12) only the portion of the rostrum anterior to P3 appears to be scalloped, while posterior to this the lateral margin is essentially straight. The holotype of *J. hunderi* (NMV P216929) has a linear (unscalloped) lateral margin of the entire maxilla.

A distinct antorbital process marks the posterolateral corner of the maxilla of *A. weltoni* and is bordered anteriorly by a deep sulcus forming the antorbital notch. The antorbital process of the maxilla is thin anteroposteriorly and thicker dorsoventrally. Posteriorly, the antorbital process overlaps and wraps around the large lacrimal, which is dorsally exposed. This appears to be the condition in all aetiocetids.

A series of dorsal infraorbital foramina are exposed on the medial half of the right maxilla above the level of M2 (Fig. 1A). The surface of the maxilla is elevated here and faces anterolaterally relative to the more horizontally orientated surface of the main rostral portion of the maxilla. A primary pair of infraorbital foramina is dorsally placed and positioned behind and above two or possibly three additional, smaller foramina. Posterodorsal crushing, however, in this region makes unclear the exact number of foramina present. The primary dorsal infraorbital foramina are approximately 4 mm in diameter and lie 8–12 mm below the premaxilla/maxilla suture on the elevated maxillary surface. CT imaging reveals a major branching of the infraorbital canal within the maxilla at this position. The infraorbital canal transmits cranial nerve V_2 from the orbit to the face and lips. A similar pair of foramina occurs in this position on the left and right maxillae in *A. cotylalveus*. In *Chonecetus goedertorum* (LACM 131146) a single, large-diameter dorsal infraorbital foramen occurs here and is associated with three other foramina located anterior to and/or below the primary foramen. CT imaging of UCMP 122900 reveals a second branching of the infraorbital canal at this same position (approximately 25 mm anterior to the primary foramina), which is the location of at least two accessory infraorbital foramina and their associated anteriorly direct sulci. Internally, the infraorbital canal continues anteriorly for another 20 mm where it crosses the maxilla–premaxilla suture and extends into the premaxilla.

The posterior opening of the infraorbital canal (i.e. the internal maxillary foramen) is well exposed in the maxilla on the anterior wall of the right orbit in UCMP 129900 and occupies a position similar to that noted in *Dorudon* (Uhen, 2004). In *Aetiocetus weltoni*, however, the foramen is much larger in diameter and is bounded below by a broad, edentulous infraorbital plate of the maxilla. As noted by Fordyce & Muizon (2001), the edentulous infraorbital plate is a diagnostic feature of mysticetes. The posterior margin of the infraorbital plate in *Aetiocetus weltoni* is evenly curved and lacks the prominent posteromedial process seen in later diverging mysticetes (e.g. balaenopterids). An evenly curved posterior margin (posteriorly concave) is also seen in most 'cetotheres'.

In *Dorudon* the horizontal portion of the maxilla forming the floor of the infraorbital canal is narrow and supports the M1-2 tooth row (Uhen, 2004). In both *Dorudon* and *Aetiocetus* spp. the posterior terminus of the maxilla reaches to the centre of the orbit where its lateral margin is first underlapped and then overlapped by the delicate jugal. The infraorbital plate of the maxilla in species of *Aetiocetus* and *Janjucetus* is edentulous, in contrast to the toothed con-

dition in basilosaurid archaeocetes (e.g. *Zygorhiza* and *Dorudon*; Kellogg, 1936; Uhen, 2004).

On the palate the maxillae meet tightly at the midline (Figs 1B, 3) and appear to be fused for most of their length in contrast to the condition in modern mysticetes where the medial borders of the maxillae are distinctly separate and expose the underside of the median rostral 'gutter' of the vomer for their entire length. Anteriorly, the maxillae are separated to expose the vomer in the palatal window described above. The anteromedial corner of the maxilla is developed as a narrow longitudinal ridge closely appressed to a similar ridge on the palatine process of the premaxilla. The anterior tip of the maxilla extends to the level of I3 (to the level of the I3-I2 diastema in *Aetiocetus cotylalveus*). From this point the border of the maxilla extends posterolaterally and passes through the middle of the I3-C diastema between and onto the dorsal surface of the rostrum.

On the palate of *A. weltoni* both maxillae are generally planar transversely and not divided into right and left longitudinal 'gutters' as in adult extant mysticetes. Interestingly, the palate of fetal balaenopterid mysticetes is also flat and does not begin to acquire the characteristic longitudinal 'gutter' until near term (Ridewood, 1923). In *Aetiocetus weltoni* a broad, shallow and generally oval fossa occurs on the posterolateral portion of each maxilla adjacent and medial to M1-3. This posterolateral fossa is bounded posteriorly by the oblique maxilla–palatine suture and medially by a broadly arched palatal convexity centred on the midline. Anteriorly, the fossa merges gradually with the planar surface of the palate. Whether or not the posterolateral fossa is homologous to the longitudinal 'gutter' of later diverging, baleen-bearing, edentulous mysticetes is unclear.

The arrangement of palatal foramina on the maxilla is complex (Fig. 3). The most posterior foramina occur at the level of M3 and are located within 16 mm of the midline. These palatine foramina (one right and one left) open anteriorly and are of small calibre (less than 2 mm diameter). Anterior to these at the level of the M1-2 diastema is a pair of larger palatine foramina (one right and one left); the right foramen is positioned more posteriorly than the left and occurs 14 mm from the midline. The left foramen occurs 12 mm anterior to the right and is positioned approximately 11 mm from the midline. Both foramina open anteriorly into broad palatine sulci that extend anteriorly to at least the level of P1. Together these four foramina appear to be homologous to typical mammalian major palatine foramina. If correct, this homology suggests that the foramina provided passage for the descending palatine artery and greater palatine nerve.

In contrast to the medially positioned major palatine foramina are a series of delicate foramina occurring on the lateral half of the maxilla (Figs 3, 5). These lateral palatal foramina are closely associated with the maxillary dentition and may be homologous with the foramina for transmission of blood (superior alveolar artery) and innervations (superior alveolar nerve) to the baleen racks in edentulous mysticetes. The series of eight lateral nutrient foramina occurs slightly medial to the left toothrow between C and M2 (the right dentary is still articulated with the skull and obscures the right side of the palate). The following description of foramina begins with the posteriormost foramen (#1) and proceeds to the anteriormost foramen (#8). Foramen #1 is small (~1 mm diameter), located approximately 10 mm from the medial alveolar margin of M2, and opens into a fine, anterolaterally orientated sulcus ~11 mm in length that forms an angle of ~40° with the sagittal plane. Anterior to foramen #1, two foramina of the same small diameter (~1 mm) are positioned ~3 mm from M1. The posterior foramen of this pair (#2) and its sulcus (~2.5 mm long) form an angle of ~60° with the sagittal plane, while the other foramen (#3) occurs 6 mm anterior to #2 with an anteriorly directed sulcus (~6.5 mm long) that is angled ~25°. Another pair of small (~1 mm diameter) foramina (#4 and #5) occur approximately 9 mm from the medial corner of P4. Sulci associated with these delicate foramina form angles of ~20° and measure ~8.5 and 5.6 mm, respectively. A larger foramen (#6) ~1.5 mm in diameter is positioned ~7 mm from the posteromedial corner of the exposed P3 root, and the associated sulcus (~15.5 mm long) forms an angle ~10° to the sagittal plane. Another large foramen (#7) is ~2 mm diameter and occurs within 4 mm of the medial alveolar border adjacent to P2. The associated sulcus of this foramen is shorter (~7 mm long) and less distinct relative to those associated with the more posterior foramina and is roughly parallel to the sagittal plane. The anteriormost foramen (#8) occurs ~3 mm medial to the diastema between C and P1. This foramen is of small calibre (~1 mm diameter), and its associated sulcus is poorly formed and orientated roughly parallel to the sagittal plane.

Delicate lateral nutrient foramina and sulci of similar size and orientation were also observed in two other Oligocene aetiocetids, *Aetiocetus cotylalveus* and *Chonecetus goedertorum*. Unfortunately, preservation in these specimens was not as good as in the holotype of *A. weltoni*. Only one obvious foramen is preserved on the palate of *A. cotylalveus* (USNM 25210) and occurs on the right maxilla adjacent to the P4-M1 diastema and 3 mm from the medial margin of the M1 alveolus. The sulcus associated with this foramen forms an angle of ~5° with

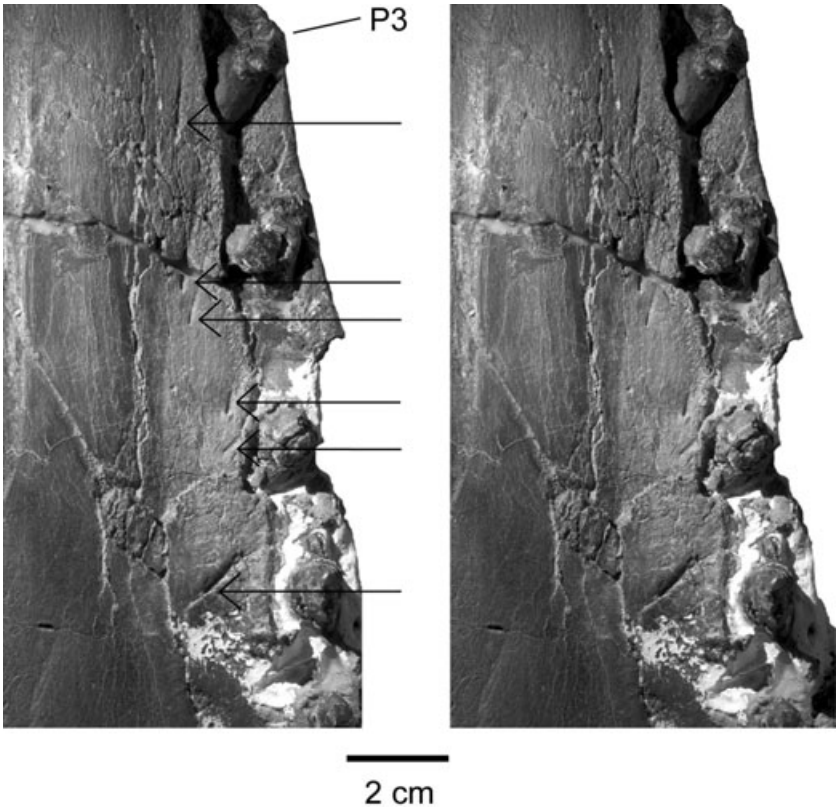

Figure 5. *Aetiocetus weltoni*, UCMP 122900, holotype; stereophotographs of portion of left palate showing location of lateral palatal foramina and sulci.

the sagittal plane and measures ~12.8 mm in length. The holotype of *Chonecetus goedertorum* (LACM 131146) preserves three obvious lateral palatal foramina. One on the right maxilla between the P2 and P3 alveoli is matrix filled and opens anteriorly into a delicate sulcus orientated ~4° to the sagittal plane. This tiny (~1 mm diameter) foramen lies ~2–3 mm from the medial margins of the adjacent alveoli. A second foramen occurs on the left maxilla adjacent to the P4 alveolus and ~1 mm from its medial margin. The associated matrix-filled sulcus measures ~7 mm in length and is orientated in the parasagittal plane. The third foramen is problematic, but occurs on the left maxilla adjacent to the M2 alveolus. The matrix-filled sulcus is orientated ~40° to the sagittal plane and measures ~5 mm in length. Recently, Sawamura *et al.* (2006) noted the presence of lateral nutrient foramina in close association with the molar and premolar dentition in a new, undescribed species of *Morawanocetus* from the late Oligocene of Hokkaido, Japan.

In UCMP 122900 the alveolar region of the maxilla is clearly defined and has distinct medial and lateral margins (Fig. 5). The medial margin locally forms a sharply elevated rim immediately adjacent to the roots of the canine and postcanine teeth. This sharp rim diminishes anteriorly becoming indiscernible within the intervening diastemata. Emlong (1966) mentions similar structures on the medial margins of the alveoli in *A. cotylalveus* (USNM 25210). The lateral margin of the alveolar region of the rostrum is coincident with the lateral edge of the premaxilla and maxilla. In fetal skulls of modern balaenopterids the medial and lateral margins of the ephemeral alveolar groove occupy similar and homologous positions on the rostrum (Ridewood, 1923). In *Aetiocetus weltoni* conspicuous embrasure pits (not seen in USNM 25210) occur between C and P1, P1 and P2, and P2 and P3; the posteriormost embrasure pit is the deepest and broadest. The diastema between P3 and P4 lacks an embrasure pit. The postcanine teeth are emergent, with the crowns well clear of their alveoli. Emlong (1966) noted the same condition in USNM 25210 and speculated that the postcanine teeth of *A. cotylalveus* were less firmly planted in the maxilla than the anterior teeth. Rostral diastemata in UCMP 122900 vary in length as follows: I1-2 ~13 mm, I2-3 ~21 mm, I3-C ~23 mm, C-P1 ~17 mm, P1-2 ~22 mm,

P2-3 ~ 22 mm, P3-4 ~17 mm, P4-M1 ~19 mm, M1-2 ~14 mm, M2-3 ~11 mm.

VOMER

On the anterior portion of the palate the vomer is exposed behind the palatine processes of the premaxillae in a small slit-like palatal window, as previously described (Fig. 3). This vomer exposure extends from the P2-3 diastema to the level of P1. *Janjucetus hunderi* has a longer vomer exposure that extends from the P2-3 diastema to the level of the canine. In *A. weltoni* (also *A. cotylalveus*) the premaxillae form the anterior border of the palatal window, while in *J. hunderi* the vomer exposure apparently is formed entirely by the maxillae. Palatal exposures of the vomer have not been reported in any other known fossil or living edentulous mysticete, nor in basilosaurid archaeocetes. Fordyce (1994, 2002), however, reported probable homologous structures on the palates of two Oligocene odontocetes. In *Simocetus rayi* the palatal window extends from approximately the P2-3 diastema to a point anterior to C, while in *Waipatia maerewhenua* the palatal window is more posteriorly placed and reminiscent of the condition in extant odontocete cetaceans (e.g. delphinoids).

As revealed by CT imaging of UCMP 122900 the vomer in the floor of the mesorostral groove terminates anteriorly approximately 88 mm behind the tip of the rostrum. From here to a point approximately 134 mm behind the rostral tip the vomer rests loosely on the premaxillae and is then exposed for 60 mm in the palatal window. Over its anterior 140 mm the vomer is a simple flattened trough. Posterior to this point the lateral margins of the vomer become progressively thickened and interlock with the adjacent maxillae along a chevron-shaped contact. The mesorostral groove extends posteriorly well into the internal narial passage where it eventually terminates, presumably against the mesethmoid. Within the internal nares the ventral portion of the vomer develops into a delicate vomerine crest that descends to the level of the ventral surface of the palatines. More posteriorly the vomerine crest becomes transversely expanded, with a maximum transverse width of 4–5 mm. This expanded portion of the vomerine crest extends posteriorly to just behind the posterior termination of the pterygoid hamuli. From this point the vomerine crest narrows to a sharp keel and ascends posterodorsally to the basicranium where it terminates within 2 mm of the vomer–basioccipital suture at a level between the midpoints of the tympanic bullae. The horizontally orientated posterior nasal plate of the vomer broadly underlaps and obscures the fused basioccipital/basisphenoid suture.

PALATINE

Both palatines are preserved in UCMP 122900, the right more completely than the left. Although crushed slightly at the midline, the palatines appear to have formed a relatively planar surface on the palate. Their contact in the sagittal plane is tight, completely concealing the vomer. Whether or not the interpalatine suture was fused is unclear, although it appears to be fused in the holotype of *A. cotylalveus* (USNM 25210). The posterior border of the palatine has a complex and unique morphology and is retracted medially to form the anterior border of the internal nares (Figs 3, 6). A narrow sliver of the palatine extends posteromedially along the deep, ventrally flattened vomerine crest to create a W-shaped suture between the palatine and vomer. The anterior margin of the internal nares is thus formed by the palatine, which is roughly orientated transverse at this level and extends 15 mm laterally to a point where the margin abruptly turns posteriorly to underlap the anterior root of the pterygoid hamulus. The palatine here forms a lobate posterolateral projection, which covers the anterior portion of the pterygoid. The lateral margin of this projection forms the palatine–pterygoid suture, which is orientated anterolaterally and crosses onto the temporal wall where it terminates at the ventral margin of the large orbital fissure. This complex contact between the palatine and pterygoid is noteworthy as it involves a squamous suture medially on the palate and a serrated suture laterally on the temporal wall. A sharp lateral crest on the palatine roughly parallels but is positioned approximately 12–15 mm medial to the oblique pterygoid–palatine suture. The apex of this palatal crest diminishes in size posteriorly and merges almost imperceptibly with the surface of the palatine at its termination on the posterolateral projection. Similar palatal crests occur in the same position on the holotype skulls of *Aetiocetus cotylalveus*, *A. polydentatus* and *A. tomitai*. Although the holotype of *Chonecetus goedertorum* does not preserve lateral palatal crests, it does possess posterolateral projections as noted by Barnes *et al.* (1995). These projections are more delicate and elongate, in contrast to the shorter and lobate projections in species of *Aetiocetus*.

The maxilla–palatine suture has been affected by crushing in the holotype skull of *Aetiocetus weltoni*, but appears to have roughly the same orientation as noted by Emlong (1966) in *A. cotylalveus*. Anteriorly, the suture is broadly convex, while laterally it curves posteriorly to contact the posterior margin of the infraorbital plate ~70 mm from the midline (60 mm in USNM 25210). The palatines are exposed on the ventral portion of the temporal wall and form the lower rim of the large orbital fissure (Fig. 7).

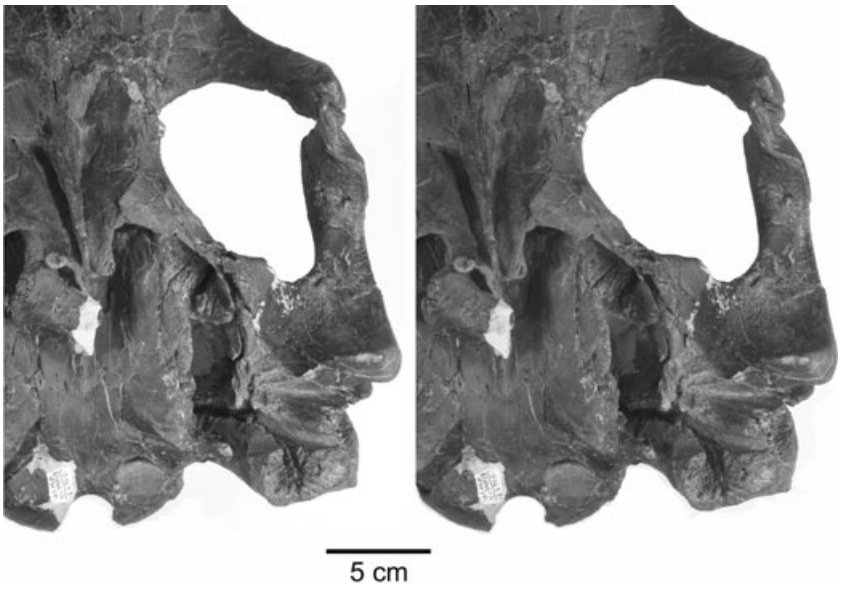

Figure 6. *Aetiocetus weltoni*, UCMP 122900, holotype; stereophotographs of left portion of basicranium and posterior region of palate.

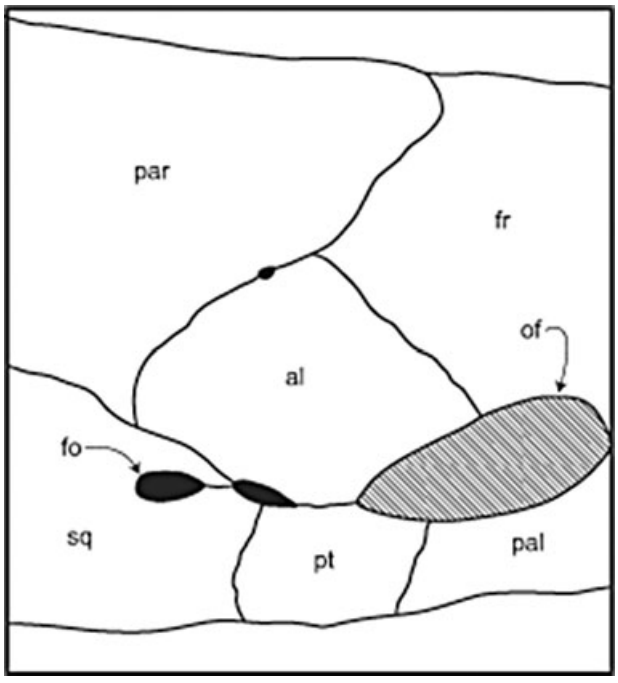

Figure 7. *Aetiocetus weltoni*, UCMP 122900, sketch of right temporal wall showing configuration of cranial elements. al = alisphenoid, fo = foramen pseudovale, fr = frontal, of = orbital fissure, pal = palatine, par = parietal, pt = pterygoid, sq = squamosal.

NASAL

The nasals are narrow, elongate and roughly rectangular elements (Figs 1A, 2), as noted by Barnes *et al.* (1995), with tightly fused internasal and nasal–premaxilla sutures. Anteriorly, the combined nasals measure ~40 mm transversely, compared with 37 mm in *Aetiocetus cotylalveus* (USNM 25210) and 53 mm in *A. polydentatus* (AMP12). Posteriorly, the nasals gradually taper in width to a minimum of 25 mm as measured 25 mm anterior to their posterior termination. In *A. polydentatus* the nasals are rather uniformly broad for their anterior 66 mm, but abruptly decrease in width to 37 mm behind this point. The anterior border of the nasals is broken in the holotype of *A. weltoni*, but appears to have been anteriorly concave. The dorsal surface of the nasals is fairly uniform in profile for most of the combined length, but is abruptly deflected dorsally in its anterior 20–25 mm. A similar dorsal deflection characterizes the nasals of *A. polydentatus* and both may be the result of post-depositional deformation. As previously mentioned, the anterolateral corner of the nasal is marked by a rugose process that is divided by the nasal–premaxilla suture. In the holotype of *Janjucetus hunderi* the nasals, although incomplete anteriorly, appear to have been generally rectangular in outline (Fitzgerald, 2006), but shorter relative to species of *Aetiocetus*.

FRONTAL

The laterally extended supraorbital process of the frontal is not depressed below the vertex, but instead lies in nearly the same plane as the cranial vertex (Fig. 1C). This is the primitive condition shared with archaeocetes, other toothed mysticetes (e.g. *Janjucetus*

and *Mammalodon*) and stem edentulous mysticetes (e.g. *Eomysticetus*). Unlike archaeocetes, however, the supraorbital process in species of *Aetiocetus*, *Janjucetus*, *Mammalodon* and *Eomysticetus* is broadly overlapped by the posteromedial portions of the rostral bones (nasal, premaxilla and maxilla). In *Aetiocetus weltoni* and *A. cotylalveus* there are well-developed preorbital and postorbital processes of the frontals that are separated by a laterally concave (in dorsal aspect) orbital rim. In contrast, the orbital rim in *A. polydentatus* is only slightly concave. In lateral aspect the orbital rim is distinctly arched in all species of *Aetiocetus*, and although the orbit diameters (OD) are impressive in size; when compared with CBL they are relatively smaller than in *Janjucetus* (OD/CBL = 12% in *Aetiocetus weltoni* compared with 24% in *Janjucetus hunderi*; Fitzgerald, 2006). It should be noted that comparing OD to CBL in *J. hunderi* might be misleading because of this taxon's uniquely shortened rostrum. A more accurate metric might be to compare OD with occipital condyle width (ODW), but unfortunately the occipital condyles are not preserved in the holotype of *J. hunderi*. Another possible metric would be comparison of OD with zygomatic width (ZW). Using this metric *J. hunderi* still has relatively larger orbits (OD/ZW = 27% in *A. weltoni* vs. 36% in *J. hunderi*), although not as markedly large as implied by the OD/CBL metric.

A well-developed temporal crest occurs on the posteromedial border of each supraorbital process in *Aetiocetus weltoni* (as noted by Barnes *et al.*, 1995), but does not extend onto the postorbital process (Fig. 1A). The right and left temporal crests converge posteromedially to merge with the sagittal ridge on the parietal. Although the frontal–parietal (coronal) suture on the vertex is somewhat difficult to interpret because of minor deformation, the configuration of this suture appears to be broadly M-shaped as described below for the parietal. Laterally, the coronal suture ascends the temporal wall nearly vertically from the alisphenoid until a level approximately 25 mm below the cranial vertex at which point the suture begins to slope anteriorly to intersect the temporal crest. From here the suture turns medially to follow the ridge of a smaller coronal crest and then turns and converges posteromedially at the midline with a similar coronal crest on the other side. These coronal crests create a conspicuous V-shaped sulcus in the frontal on the vertex of the skull (Fig. 2) and may be age-related features.

The frontal exposure on the vertex is rather short, measuring ~20 mm in the anteroposterior dimension. In the holotype of *Aetiocetus cotylalveus* the frontal exposure is longer, measuring ~60 mm in the anteroposterior dimension. This same measurement in the holotype of *A. polydentatus* is only about 15 mm. Although not clearly described by Fitzgerald (2006), the frontal exposure in *Janjucetus* appears to be relatively long (~100 mm).

In the holotype of *Aetiocetus weltoni*, several small calibre supraorbital foramina occur on the medial portion of the frontal. The posteriormost foramen is located within 9 mm of the frontal–maxilla suture. Anterolateral to this single foramen is a closely positioned pair of supraorbital foramina on the right frontal that lie within 15 mm of the frontal–maxilla suture. On the left frontal only a single anterior foramen is preserved and is located approximately 16 mm from the suture. *Chonecetus goedertorum* has a greater number of supraorbital foramina, many of which are associated with distinct, but delicate, elongate sulci.

On the ventral surface of the supraorbital process of the frontal the optic canal is broad and poorly defined and occupies most of the exposed ventral surface. The long axis of the optic canal forms an anterolaterally directed angle of approximately 45° to the sagittal plane. The distinct dorsal and ventral orbital crests noted in *Dorudon* by Uhen (2004) are absent in aetiocetids, although such crests do occur in most fossil and living edentulous mysticetes (e.g. *Aglaocetus*, *Diorocetus*, *Parietobalaena*, *Balaenoptera* and *Eschrichtius*). A number of frontal foramina occur on the roof of the optic canal near its middle. Anteriorly, the frontal forms a long transverse suture with the lacrimal. Anteromedially, the frontal forms an obscure contact with the orbitosphenoid, although the configuration of this bone is poorly defined. Posteromedially, the frontal forms the roof and anterior margin of the large orbital fissure.

Pterygoid

The lateral pterygoid lamina in *Aetiocetus weltoni* (UCMP 122900) is exposed for 23 mm on the medial wall of the temporal fossa where it forms a complex, almost foliate suture with the falciform process of the squamosal (Fig. 7). The foramen pseudovale does not involve the pterygoid, but is instead confined to the squamosal. Dorsally, the lateral pterygoid lamina forms a relatively horizontal butt joint with the alisphenoid. The anterodorsal corner of the pterygoid forms the posteroventral margin of the large oval orbital fissure (Fig. 7). Anteriorly, the lateral pterygoid lamina has a foliate sutural contact with the palatine.

On the palate the contact of the pterygoid with the palatine is unusual as already discussed. The pterygoid hamulus is distinctly elongate and developed as a transversely broad, but dorsoventrally thin, spatulate process (Figs 3, 6). The posterior 60% of the hamulus is finely roughened on its ventral surface,

the pattern being reminiscent of scars left by Sharpey's fibres at muscle insertions. Diagenetic distortion in this area has narrowed the internal narial opening and forced the hamuli to impinge medially on the vomer. Figure 3 depicts the reconstructed morphology of the internal narial region, which consists of elongate slit-like choane divided medially by the ventrally flared vomerine crest. The anterior margin of the internal narial opening is formed by the palatine, while the lateral margin is formed by the pterygoid hamulus. The holotype of *A. cotylalveus* is also distorted in this region, but appears to have the same general morphology. Emlong (1966) erroneously identified the pterygoid hamuli of *A. cotylalveus* as the 'transversely narrowed posterior ends of the palatines' (p. 12). This error led Emlong and later Kellogg (1969) to incorrectly conclude that the internal nares opened far posteriorly at the level of the pterygoid sinus fossa rather than at the level of the temporal fossa. The holotype of *A. polydentatus* (AMP 12) is essentially undistorted in this region and preserves well-defined, slit-like internal narial openings bordered laterally by elongate pterygoid hamuli. Unfortunately, this morphology is not adequately represented in the published illustrations and photographs of AMP 12.

The deeply bifurcated internal narial opening found in species of *Aetiocetus* represents a unique morphological feature that is not shared with any other known toothed or edentulous mysticete. It should be noted, however, that the condition in species of *Chonecetus* is currently unknown due to the lack of preserved pterygoids.

The pterygoid sinus fossa (anterior pterygoid sinus of Luo & Gingerich, 1999), as prepared on the left side of UCMP 122900, is deep and ovoid and is constructed as in later diverging mysticetes from the lateral, medial and superior pterygoid laminae (Fig. 6). This is similar to the condition in basilosaurids and differs slightly from the condition in stem odontocetes where the roof of the pterygoid sinus fossa is formed by the superior pterygoid lamina plus portions of the alisphenoid and basisphenoid (Luo & Gingerich, 1999). In *Janjucetus* the superior pterygoid lamina does not completely cover the medial portion of the alisphenoid (Fitzgerald, 2006) and thus the roof of the pterygoid sinus fossa is formed from alisphenoid posteriorly and pterygoid anteriorly. Unfortunately, the construction of the pterygoid sinus fossa in eomysticetids and the stem 'cetothere' *Micromysticetus* is currently unknown due to poor preservation of this region in the respective holotype specimens.

In extant mysticetes the pterygoid sinus fossa is enlarged anteriorly within the pterygoid bone and is floored in part by the pterygoid hamulus. This advanced condition is not seen in *Aetiocetus weltoni* where the pterygoid sinus fossa is more open ventrally and not floored by any part of the pterygoid.

In *Aetiocetus weltoni* the surface of the superior pterygoid lamina forming the roof of the pterygoid sinus fossa has a rugose surface texture. A distinct sulcus for the mandibular branch of the trigeminal nerve obliquely crosses the posterolateral corner of the superior pterygoid lamina to exit through the foramen psuedovale. This condition is similar to that described in adult basilosaurids (Luo & Gingerich, 1999). In *Aetiocetus weltoni* the posterior portion of the lateral pterygoid lamina is overlapped externally by the falciform process of the squamosal. In addition, the posterolateral corner of the superior pterygoid lamina behind the trigeminal sulcus underlaps and obscures the anterior process of the petrosal. Medially, the pterygoid sinus fossa is coincident with the anterior portion of the peribullar sinus, which is excavated into the dorsolateral portion of the medial pterygoid lamina. The posterior portion of the peribullar sinus appears to extend slightly onto the lateral edge of the basioccipital above the basioccipital crest. The posterior pterygoid lamina (vaginal process) is transversely broad and extends posteriorly to cover the basioccipital–basisphenoid suture. The posterior pterygoid lamina thus terminates at the level of the postglenoid process of the squamosal. The suture between the posterior pterygoid lamina and the nasal plate of the vomer is parasagittally orientated and overrides the anterior edge of the basioccipital crest.

Lacrimal

The lacrimals are well preserved in *Aetiocetus weltoni* and project laterally beyond the external surfaces of the preorbital process of the frontal and the antorbital process of the maxilla. Unlike the lacrimal in extant mysticetes, which consists of a relatively small, flattened bone loosely situated between the preorbital process of the frontal and the antorbital process of the maxilla, the lacrimal of *A. weltoni* is intimately joined in articulation with the maxilla and frontal. In dorsal aspect the lacrimal has a large, narrowly oval exposure at the back of the rostrum and deeply invades the lateral margin of the base of the ascending process of the maxilla (Figs 1A, 2). The lacrimal exposure on the left side measures ~72 mm in the transverse dimension and is slightly depressed below the level of the adjacent frontal and maxilla.

The rounded medial portion of the lacrimal in UCMP 122900 is ~17 mm in anteroposterior diameter and distinctly broader than the lateral portion, which measures only 8.5 mm in the same dimension. The anterior margin of the lacrimal is overlapped along a transversely elongate scarf joint by the prominent antorbital process of the maxilla. The maxilla forms

a sharp transverse crest in this region, whereas medially the maxilla–lacrimal contact is flattened and more subdued. Posteriorly, the maxilla–lacrimal contact is only ~20 mm in transverse length before it terminates at the base of the ascending process of the maxilla. From this point the lacrimal continues laterally and wraps around the preorbital process of the frontal. Here the lacrimal narrows as it is pinched between the preorbital process of the frontal and the antorbital process of the maxilla. As mentioned, the lateral border of the lacrimal extends beyond both of these processes and is developed as a rugose projection that is anteroposteriorly narrow and dorsoventrally elongate. Within the orbit the lacrimal has a relatively large exposure where it forms a deeply serrated suture with the frontal. There is no evidence of a lacrimal canal, although this area is not well preserved in UCMP 122900.

A similar lacrimal with large dorsal exposure that deeply invades the maxilla occurs in *Aetiocetus cotylalveus* (USNM 25210), *A. polydentatus* (AMP 12) and *Chonecetus goedertorum* (LACM 131146). Emlong (1966) briefly described the large lacrimal of *A. cotylalveus* and illustrated it (fig. 4). Barnes *et al.* (1995), however, did not mention the lacrimal in their descriptions of aetiocetids and omitted this bone from their skull reconstructions. As reported by Fitzgerald (2006) the lacrimal of *Janjucetus hunderi* is enlarged both posteromedially and anterolaterally and parallels the anterior edge of the supraorbital process of the frontal. Overall the lacrimal is thick and rod shaped and restricted to a level below the surface of the supraorbital process, anteroposteriorly. In *Dorudon atrox* the lacrimal is small and largely concealed dorsally by the frontal. The large rostral exposure of the lacrimal appears to be a feature unique to aetiocetids and has not been reported in any previously described archaeocetes, odontocetes or mysticetes.

JUGAL

Portions of both jugals are preserved in UCMP 122900. The right jugal is more complete anteriorly and is a delicate strut-like element closely appressed to the infraorbital plate of the maxilla. Although the anterior contact of the jugal is obscured by crushing on this side, it appears that the jugal underlies the extreme posterolateral corner of the infraorbital plate, but quickly crosses anteriorly over onto the dorsal side of the infraorbital plate to become sandwiched between the maxilla and the lacrimal. On the left side, only the posterior end of the jugal is preserved. This narrow, spatulate remnant is broadly overlapped by the anterior tip of the zygomatic process of the squamosal (Fig. 6) to create a scarf joint 41 mm in length. The jugal here measures only 10 mm in transverse width and 7–8 mm in dorsoventral thickness, and is lodged in a narrow facet on the anteroventral corner of the zygomatic process. Overall, the jugal is a rather delicate, strap-like element with a relatively short articulation with the anteroposterior tip of the zygomatic process of the squamosal. Emlong (1966) erroneously considered the jugal of *A. cotylalveus* to be sandwiched between the zygomatic process of the squamosal and the postorbital process of the frontal. His error was probably due to post-depositional distortion in USNM 25210. As reported by Fitzgerald (2006) *Janjucetus hunderi* has a thick and sturdy jugal that underlaps the extreme anterior tip of the zygomatic process. Although the anterior 60% of the jugal of *Dourdon atrox* is also strap-like, the posterior portion of the jugal has a much longer and more robust articulation with the zygomatic process (Uhen, 2004).

PARIETAL

The parietal is incompletely preserved in UCMP 122900 and is missing the posterodorsal portion on the vertex. In lateral aspect the dorsal surface of the parietal on the vertex is at the same level as the frontal and was presumably only slightly below the level of the apex of the supraoccipital as in the holotype of *Aetiocetus polydentatus* (AMP 12). The distinctly depressed position and dorsally concave profile of the parietal in the holotype of *A. cotylalveus* (USNM 25210) may be the result of post-depositional deformation. The undistorted parietal in *Janjucetus hunderi* appears to represent the generalized condition in toothed mysticetes (i.e. frontal and parietal at same level and close to level of apex of supraoccipital).

In UCMP 122900 the squamosal–parietal and alisphenoid–parietal sutures on the left temporal wall are distinct. The parietal–frontal (coronal) suture, however, is partially obscured. On the vertex, the coronal suture is broadly M-shaped, with a narrow sliver of frontal extending posteriorly between the lobate anterior wings of the parietals (Fig. 2). A similar narrow frontal sliver occurs in *A. polydentatus* (AMP 12). In *A. cotylalveus* (USNM 25210) the posterior frontal extension is transversely broader between the lobate anterior wings of the parietals. The coronal suture in *Chonecetus goedertorum* (LACM 131146) is roughly W-shaped with a bifid posterior frontal extension divided by a short anterior parietal extension. In this taxon the anterior wings of the parietals are sharply angular rather than lobate (Barnes *et al.*, 1995: fig. 10). The coronal suture in *Janjucetus hunderi* also has sharply angular anterior wings of the parietals, but lacks the bifid posterior

frontal extension (Fitzgerald, 2006, electronic supplement, fig. S3).

Although most of the supraoccipital shield in UCMP 122900 is missing (and thus the occipital–parietal suture), the degree of parietal exposure on the vertex can be estimated at 65 mm if the lobate anterior wings of the parietals are included. If only the medial posteriorly retracted region of the parietals at the midline is considered, the degree of parietal exposure is estimated at 40 mm. In *Aetiocetus cotylalveus* the maximum and minimum parietal exposures are 61.8 and 34.5 mm, respectively. The minimum parietal length roughly corresponds to the preserved length of the low sagittal ridge in UCMP 122900. Both *A. cotylalveus* (USNM 25210) and *A. tomitai* (AMP 2) have a flattened cranial vertex with no sagittal ridge or crest, while *A. polydentatus* (AMP 12) has a very short sagittal crest measuring ~10 mm in length that descends sharply from the apex of the supraoccipital to the vertex. Although broken posteriorly, a distinct sagittal ridge (measuring at least 14 mm in length) does occur in UCMP 122900 and is broadly triangular in cross-section in contrast to the narrower (and shorter) sagittal crest in *A. polydentatus*. *Janjucetus hunderi* (NMV P216929) has a distinct, low sagittal crest (Fitzgerald, 2006) that extends nearly the full length of the parietal (~80 mm).

In *A. weltoni* the transverse width of the parietal across the intertemporal region is relatively narrow (68 mm) and broadly rounded as in archaeocetes. In *A. cotylalveus*, *A. tomitai* and *Janjucetus hunderi* the cross-sectional shape of the intertemporal region is similar, although distinctly broader (85, 86 and ~80 mm, respectively). In *A. polydentatus* the parietals are marked by distinct laterally placed temporal crests that diverge anterolaterally towards the supraorbital processes of the frontals. These crests come to within 20 mm of each other at the apex of the supraoccipital, but do not meet. Lateral to these crests, the parietal wall in *A. polydentatus* is nearly vertical giving the intertemporal region a squared-off cross-section in contrast to the more ovoid cross-sectional shape seen in other species of *Aetiocetus* (e.g. *A. weltoni*, *A. cotylalveus* and *A. tomitai*). *Janjucetus* and *Mammalodon* appear also to possess the ovoid cross-section (Fitzgerald, 2006). In this light the conclusion by Geisler & Sanders (2003) that an ovoid cross-sectional shape of the parietals is an aetiocetid synapomorphy is in error. These authors also suggested that aetiocetids lacked a sagittal crest.

SUPRAOCCIPITAL

The anterior 60% of the supraoccipital shield in *Aetiocetus weltoni* (UCMP 122900) is missing and only the region immediately dorsal to the foramen magnum is preserved. The morphology of this region suggests that the shield was rather vertically orientated posteriorly and abruptly inclined anteriorly as also observed in *A. cotylalveus* (USNM 25210) and *A. polydentatus* (AMP 12). In both of the latter specimens a distinct external occipital crest is preserved at the midline on the dorsal region of the supraoccipital. On either side of this central occipital crest, near the dorsolateral margins of the shield, is an elevated, semicircular, rugose boss for attachment of the neck extensor musculature. Between the muscle attachment and the occipital crest the surface of the shield is depressed to form right and left concave embayments. It is assumed that these features of the supraoccipital shield as preserved in the holotypes of *A. cotylalveus* and *A. polydentatus* were also present in *A. weltoni*.

More posteriorly on the right side of the occipital shield in UCMP 122900 is a distinct dorsal condyloid fossa (in the exoccipital) just above the dorsal margin of the occipital condyle (indistinct in USNM 25210). Similar fossae appear in this same position in *Chonecetus goedertorum* and later diverging mysticetes and have been reported in *Janjucetus hunderi* (Fitzgerald, 2006). Dorsal to these fossae in UCMP 122900 the remnant of the supraoccipital shield is nearly vertical, but becomes more anteriorly inclined toward the broken vertex. The lambdoidal crests are entirely missing except for a small remnant at the posteromedial corner of the squamosal fossa. This remnant suggests that the lambdoidal crest was rather sharp edged and extended only slightly dorsolaterally as in the holotype of *Aetiocetus cotylalveus* and unlike the condition in the holotype of *A. polydentatus* (AMP 12) where the lambdoidal crest broadly overhangs the parietal wall in the temporal fossa. In the latter taxon the occipital shield has an overall triangular shape in contrast to the more broadly arcuate shield of *A. cotylalveus* (Barnes *et al.*, 1995). *Janjucetus* and *Mammalodon* have smaller and more vertically orientated occipital shields, which like *A. polydentatus* have lambdoidal crests that flare dorsally and anterolaterally to overhang the temporal wall (Fitzgerald, 2006).

EXOCCIPITAL

Dorsally, the exoccipital–supraoccipital contact is obscure due to sutural fusion. The occipital condyles are nearly complete and have a generally reniform shape in posterior aspect. Their dorsal transverse width is greater than the ventral width. The dorsal intercondylar notch is broad and shallow, while the ventral intercondylar notch is narrower and more

recessed. The foramen magnum is broadly quadrate. The condyles occupy a short, elevated pedicle. As prepared there are no obvious condyloid foramina.

The preserved left paroccipital process is very robust (i.e. anteroposteriorly thick) (Fig. 4A). In posterior aspect the planar surface of the paroccipital process is roughly quadrate and extends ventrally to a level below the basioccipital crest. This appears to be the condition in all species of *Aetiocetus*. In *Chonecetus goedertorum*, instead, the irregular posterior surface of the paroccipital process is more delicate (i.e. anteropostiorly thin) and lobate (i.e. not quadrate) and does not extend ventral to the basioccipital crest. This appears also to be the condition in *Janjucetus hunderi*. In *A. weltoni* the ventral surface of the paroccipital process is rugose and has an anterior embayment adjacent to the well-defined sulcus for the facial nerve (Fig. 6). This anterior embayment may be homologous with the paroccipital concavity of odontocetes, which forms the posterior border of the posterior sinus as noted in archaeocetes (Oelschlager, 1986). This feature appears to be a symplesiomorphy of Cetacea although it has been erroneously regarded as a synapomorphy of the Platanistoidea + Eurhinodelphoidea + Delphinida (Muizon, 1984, 1991). The medial wall of the posterior sinus is formed by a curved portion of the exoccipital that produces a crescent-shaped margin ventrally (also observed in the holotypes of *A. cotylalveus*, *A. polydentatus* and *C. goedertorum*). A poorly formed, small bony cup near the roof of the conical posterior sinus is probably the point of articulation of the stylohyal with the exoccipital. The posterior process of the petrosal is tightly fused to the exoccipital along their mutual contact.

The portion of the exoccipital immediately lateral to the basioccipital crest is marked by an elongate finger-like projection 20 mm in length (broken in USNM 25210). Lateral to this projection is the narrow and well-defined jugular notch. Lateral to the jugular notch is the paroccipital process. There is no separate hypoglossal foramen on the ventral surface of the exoccipital. Instead, the passage for the hypoglossal cranial nerve (XII) is confluent with the posterior lacerate foramen (cranial hiatus). This is the condition in basilosaurids, mysticetes and odontocetes (Luo & Gingerich, 1999).

Basioccipital

The basioccipital is exposed for a short distance behind the posterior terminations of the pterygoid and vomer and is marked laterally by prominent, dorsoventrally thickened basioccipital crests (Fig. 6), a mysticete synapomorphy (Fitzgerald, 2006). The ventral surface of each crest is ovoid and has a rugose texture for attachment of the neck flexor musculature. The posterior border of the basioccipital crest is enlarged and roughly pyramidal in shape and projects posteroventrally beneath the posteromedial corner of the exoccipital to form a conspicuous notch between these two bones. Similar basioccipital crests occur in *Aetiocetus cotylalveus* (USNM 25210) and *A. polydentatus* (AMP 12). As noted by Fitzgerald (2006) the basioccipital crest of *Janjucetus hunderi* is more bulbous and transversely elongated along an axis parallel with the external auditory meatus. A similar condition occurs in *Morawanocetus yabuki* (AMP 1). Overall, the basioccipital in species of *Aetiocetus* is more anteroposteriorly elongate and transversely narrow.

Squamosal

A deep squamosal fossa extends from the posterior margin of the temporal fossa to the juncture between the zygomatic crest and the lambdoidal crest. This fossa is elongate in the parasagittal plane with a subtle anterolateral 'pocket' or second fossa (*fide* Barnes *et al.*, 1995). The composite squamosal fossa is bounded laterally by a thick (not keeled) zygomatic crest on the dorsal margin of the zygomatic process. A distinct prominence occurs on the posterior portion of the zygomatic crest at the back of the anterolateral pocket of the squamosal fossa. Anteriorly, the zygomatic crest aligns with the medial, rather than lateral, edge of the zygomatic process.

The zygomatic process is elongate, narrow and orientated in the parasagittal plane. In lateral aspect (Fig. 1C) the zygomatic process is thinnest near its middle and expanded both anteriorly and posteriorly. The zygomatic process is dorsoventrally thickest anteriorly as in other species of *Aetiocetus* (Barnes *et al.*, 1995). The lateral side of the zygomatic process is roughly planar, while the medial side is more convex. As mentioned previously, a distinct elongate facet is present on the ventral side of the anterolateral corner of the zygomatic process. This facet houses the narrow and spatulate posterior portion of the jugal.

The posteroexternal portion of the squamosal lateral and anterior to the exoccipital forms a rugose and posterolaterally orientated vertical platform for insertion of neck extensor muscles. Muscle insertion subdivisions are not obvious, but probably included the splenius, mastohumeralis, sternomastoideus and trachelomastoideus (Schulte, 1916). There is no well-formed post-tympanic process of the squamosal and instead this area is slightly concave and terminates ventrally against a laterally projecting posterior process of the petrotympanic complex.

Medially, the squamosal contacts the parietal on the temporal wall by a sinuous and slightly elevated

serrated suture that is dorsally arched. The suture is roughly parallel to the floor of the squamosal fossa anteriorly and rises rather abruptly posteriorly to meet the lambdoidal crest (Fig. 2). Anteriorly, the squamosal does not form a distinct pterygoid process, but instead makes a blunt, nearly vertical butt joint with the pterygoid (Fig. 7). The foramen pseudovale is ovoid and measures 13–14 mm in length and 6 mm in height. The foramen is entirely contained within the squamosal, with a delicate intra-squamosal suture extending anteriorly to the squamosal/alisphenoid suture. The falciform process broadly underlaps the foramen and terminates ~14 mm from its anterior rim. A second, but smaller (12 mm by 3 mm), narrowly ovoid foramen occurs at the apex of the falciform process in the region of the triple junction formed by the squamosal, alisphenoid and pterygoid sutures. Both foramina align along a horizontal flexure that anteriorly follows the slightly deformed pterygoid/alisphenoid suture. The homology of this foramen is uncertain.

The postglenoid process of the squamosal is directed ventrally (not posteroventrally) and tapers distally to a sharp edge (Fig. 1C). It is relatively thin anteroposteriorly, in contrast to the distally thickened postglenoid processes of more derived edentulous mysticetes. The postglenoid ridge is short and medially ascends sharply to form a premeatal crest. There is no obvious spinous process of the squamosal, as this area appears to be obscured on the left side by the crushed posterior pedicle of the petrotympanic complex. A distinct sigmoid fossa occurs on the extreme medial portion of the postglenoid ridge just lateral to the epitympanic recess on the petrosal (Fig. 6). The sigmoid fossa received the dorsal margin of the sigmoid process of the tympanic as in protocetids (Geisler & Sanders, 2003) and basilosaurids (Luo & Gingerich, 1999) and indicates a more complex articulation between the tympanic bulla and basicranium than occurs in later diverging edentulous mysticetes (i.e. three areas of articulation vs. only two). Sigmoid fossae of similar morphology occur in the holotypes of *Chonecetus goedertorum*, *C. sookensis* and *J. hunderi*. The holotype of *Aetiocetus cotylalveus* preserves the sigmoid process of the left tympanic bulla still in articulation with the sigmoid fossa of the squamosal. The presence of a spiny process of the squamosal at the squamosal–petrosal suture adjacent to the sigmoid fossa as seen in archaeocetes and stem odontocetes cannot be confirmed in *A. weltoni* due to poor preservation.

The glenoid fossa is distinctly concave and faces anteriorly, a feature consistent with that of basilosaurids and other aetiocetids and unlike the more planar and even convex glenoid fossae of later diverging edentulous mysticetes. The curvilinear length of the fossa indicates a broad articulation with the mandibular condyle and suggests a synovial temporomandibular joint. Anteromedial to the glenoid fossa the preglenoid part of the squamosal (*sensu* Luo & Gingerich, 1999) is broadly concave and extends only to the level of the foramen pseudovale. The anterolateral margin of the preglenoid region is extended into the temporal fossa as a distinct, anteriorly directed subtemporal crest (Fig. 6). This condition results in a distinct swelling (as viewed in dorsal aspect) of the squamosal at the back of the temporal fossa and in front of the squamosal fossa. Homologous anteriorly directed subtemporal crests occur in other aetiocetids and appear to be absent in *Janjucetus* and *Mammalodon*. *Zygorhiza kochii* (e.g. USNM 11962) has a broader, anteriorly orientated subtemporal crest, while in *Dorudon atrox* the large subtemporal crest is more anterolaterally directed (Uhen, 2004).

The entoglenoid region of the squamosal (*sensu* Luo & Gingerich, 1999) is well separated (i.e. ventral) from the preglenoid region, is transversely narrow and does not have a facet for articulation with the tympanic bulla (Fig. 6). In basilosaurids the entoglenoid region is anteriorly broader where it contacted the tympanic bulla (Luo & Gingerich, 1999). In *Aetiocetus weltoni* the tympanic bulla contacted the anterior process of the petrosal anteriorly, the sigmoid fossa of the squamosal medially and the posterior process of the tympanic posteriorly. This represents an intermediate condition between basilosaurids (and stem odontocetes) and later diverging mysticetes. In the latter taxa the tympanic bulla only articulates with the anterior process of the petrosal and the posterior process of the tympanic via the anterior and posterior pedicles, respectively. The entoglenoid margin in *A. weltoni* is retracted dorsally to expose the lateral portion of the anterior process of the petrosal (tegmen tympani). Similar, dorsally retracted entoglenoid margins have been reported in *Simocetus rayi* (Fordyce, 2002) and occur in *Eomysticetus whitmorei* and *Chonecetus goedertorum* (our pers. observ.).

The external auditory meatus is deeply incised between the postglenoid and posterior tympanic processes of the squamosal (Fig. 6). The latter is poorly defined because instead of a distinct posterior meatal crest there is a continuous near-vertical, planar surface extending from the squamosal onto the posterior process of the tympanic. The infundibulum of the external auditory meatus measures ~41 mm in transverse length and varies in width from 10 mm (laterally) to 5 mm (medially). Extending dorsally from the dorsolateral rim of the external auditory meatus is a smooth-sided, vertical sulcus measuring ~8 mm in width. This sulcus is deeply impressed ventrally, but dorsally merges smoothly with the lateral surface of the zygomatic crest. A similar ver-

tically orientated sulcus occurs in other species of *Aetiocetus*, as well as in species of *Chonecetus*.

Petrosal

The left petrosal is incompletely preserved and is missing essentially the entire promontorium. The anterior process is artificially bifurcated longitudinally by a fracture, but otherwise appears to be complete. It is tightly appressed to the squamosal and underlapped by the posterolateral corner of the superior pterygoid lamina at the back of the pterygoid sinus fossa. The anterior process is broad dorsoventrally (~20 mm), thin transversely (~10 mm) and measures ~23 mm in length (as preserved). A short (2 mm) remnant of the anterior pedicle occurs near the posteroventral corner of the anterior process and there is no obvious lateral tuberosity. The medial surface of the anterior process is generally smooth. A sharply defined embayment posterior to the anterior pedicle represents the mallear fossa, which is partially blocked laterally by the dislodged incus. Further preparation and removal of the incus is needed to facilitate its description. The same is true for the stapes, which is still seated in the fenestra ovalis. Anterior to the fenestra ovalis is a sharply defined groove for the tensor tympani measuring 10 mm in length. The facial sulcus is blocked anteriorly by the stapes and incus, while posteriorly the sulcus is obscured by the crushed posterior pedicle of the tympanic. The posterolateral corner of the promontorium is partially preserved including a bulbous caudal tympanic process and the floor of a crushed fenestra rotunda. The stapedial muscle fossa is obscured by the caudal tympanic process. Posterior to the caudal tympanic process the posterolaterally orientated facial sulcus is confluent dorsally with a narrow and elongate sylomastoid fossa, which does not extend onto the posterior process of the tympanic. The petrosal portion of the posterior process is difficult to distinguish from the tympanic portion due to apparent fusion of these two elements. The remnant of the crushed posterior pedicle, however, does serve as a landmark to distinguish at least a portion of the tympanic contribution to the posterior process. It is also clear that the nearly vertically orientated anterior portion of the posterior process is formed entirely by the tympanic. This vertical surface is covered by the thin posterior tympanic process of the squamosal, which defines the posterior margin of the external auditory meatus. The petrosal portion of the posterior process is marked by the shallow, smooth-walled facial sulcus, which measures 37 mm in length and averages approximately 6 mm in width. The composite posterior process is laterally elongated and terminates in a dorsoventrally flared 'mastoid' process with a rugose external surface texture. The apparent fusion of the petrosal and tympanic portions of the posterior process together with the transverse elongation of the process are viewed as derived features (see phylogenetic discussion).

As preserved, the left petrosal of *Aetiocetus weltoni* does not retain enough morphology (Fig. 6) to provide a complete understanding of the morphology of this important region. However, some useful comparisons are possible. The more complete left petrosal of *Chonecetus goedertorum* (LACM 131146) has a similar dorsoventrally broad and transversely narrow anterior process, but a shorter composite posterior process. In *C. goedertorum* the groove for the tensor tympani is less distinct, as is the mallear fossa. The promontorium is complete and its dorsoventral dimension is nearly twice that of the transverse dimension. The petrosal of *Eomysticetus whitmorei* (ChM PV4253) also has a similar shaped anterior process, but a much shorter and more odontocete-like composite posterior process. In *E. whitmorei* the petrosal and tympanic portions of the posterior process make contact along a spiraled suture and remain unfused. In addition the posterior process is not as elongate and is not fused with the adjacent exoccipital and squamosal in *E. whitmorei*. The left petrosal of *Janjucetus hunderi* is well illustrated, but largely undescribed by Fitzgerald (2006). From the published figures, however, it appears to have a similar shaped anterior process, but a relatively short posterior process.

Tympanic bulla

The left tympanic bulla of UCMP 122900 was removed from the skull for study (Fig. 8). Overall, the bulla is well preserved. The anterior pedicle is well defined, while the posterior pedicle is crushed. The dorsal edge of the lateral wall is broken and folded into the tympanic cavity and the sigmoid process is deformed posteriorly and collapsed onto the conical process (Fig. 8A).

The posterior rim of the sigmoid process is thick and broadly arched dorsally and embayed ventrally to support the tympanic membrane. The general morphology of this process closely resembles that of later diverging mysticetes. Thus, it seems that the mysticete sigmoid process is generalized and highly conserved. The left malleus is still connected to the sigmoid process by a distorted gonial process. The surfaces for articulation with the incus have been artificially rotated ~90° to face posteriorly and lie close to the sigmoid process. The conical process is relatively small and domed. The ventral base of the conical process measures approximately 13 mm anteroposteriorly, while its dorsoventral dimension

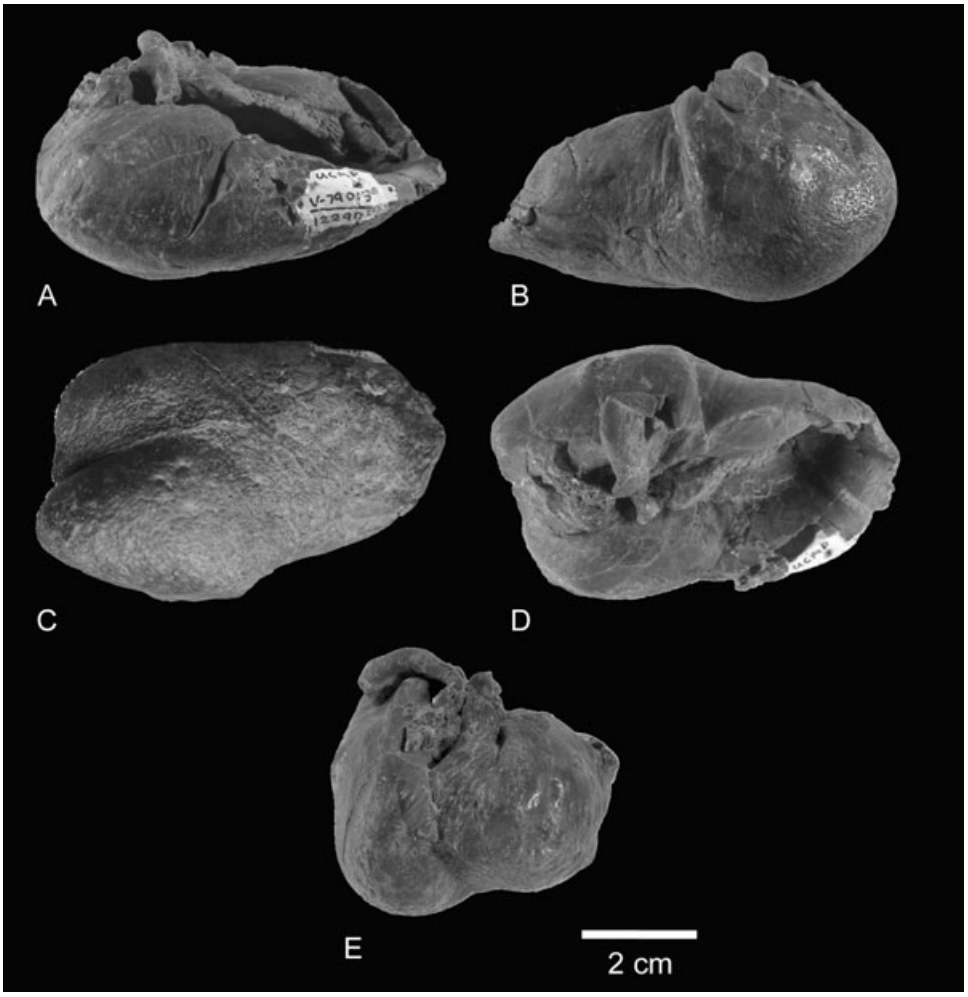

Figure 8. *Aetiocetus weltoni*, UCMP 122900, holotype left tympanic bulla. A, medial view; B, lateral view; C, ventral view; D, dorsal view; E, posterior view.

measures only about 2 mm. Posterior to the conical process is the elliptical foramen, which is obscured by the deformed posterior pedicle. Anterior to the sigmoid process on the external surface of the lateral wall is a deep lateral furrow that extends nearly to the ventral surface. The lateral wall of the bulla anterior to the lateral furrow is medially deflected relative to the lateral surface of the bulla posterior to the lateral furrow (Fig. 8B). This condition gives the bulla a distinctly broader posterior transverse width (relative to anterior width) in ventral aspect. A similar condition occurs in *Eomysticetus whitmorei* (ChM PV4253). Both taxa also preserve a weak anterior spine at the anterior margin of the bulla beneath the Eustachian notch (Fig. 8C).

The posterior margin of the bulla has a well-defined interpromontorial notch between the inner and outer posterior prominences (Fig. 8C). The outer posterior prominence is extended more posteriorly than the inner posterior prominence. The interpromontorial notch is continuous with a short, but broad median furrow, which extends midway onto the ventral surface of the bulla. The involucral ridge medial to this furrow is weakly developed (relative to the distinct involucral ridges in later diverging mysticetes) and lies nearly at the same level as the ventral bullar surface. Laterally, there is no obvious main ridge developed on the ventral surface, although the anterior extension of the outer posterior prominence could be considered a rudimentary main ridge. This subtle feature occurs near the ventrolateral border of the bulla. In posterior aspect the outer posterior prominence is smoothly globose. In contrast the inner posterior prominence is transversely broader and characterized by a distinct, transversely orientated linear ridge that extends across the interpromontorial notch to contact the posteromedial corner of the outer posterior prominence (Fig. 8D). Similar transverse

ridges occur in all species of *Aetiocetus* examined, but do not occur in *Morawanocetus yabuki* or the majority of later diverging mysticetes. However, the basal edentulous mysticete *Eomysticetus whitmorei* has a sharp transverse ridge on the inner posterior prominence as does the basilosaurid archaeocete *Zygorhiza kochii*.

The medial surface of the involucrum is broadly curved dorsoventrally and marked by poorly defined transverse creases (Fig. 8A, D). There is no obvious dorsal posterior prominence. Although the dorsal margin of the lateral wall is collapsed into the tympanic cavity, the general outline of the large and anteriorly open Eustachian notch is preserved. Internally, the tympanic cavity is divided into anterior and posterior portions by a broad, transverse median ridge. Posterior to this ridge is the involucral elevation.

The posterior process of the right bulla is solidly fused to the posterior process of the petrosal and remains in the skull. As mentioned, the right sigmoid process is articulated with the sigmoid fossa of the squamosal. Although the suture between the posterior process of the tympanic bulla and the petrosal is fused, it appears that the posterior process of the petrosal extends laterally nearly the full length of the composite posterior process

Alisphenoid

The alisphenoid on the ventral surface of the skull appears to be completely concealed by the superior pterygoid lamina in the pterygoid sinus fossa. In contrast, the alisphenoid is large and broadly exposed on the temporal wall and is not covered by the pterygoid as in later diverging edentulous mysticetes (Fig. 7). Although the alisphenoid–frontal suture is mostly obscured, the sutural contacts with the parietal, squamosal, and pterygoid are fairly well defined and serrated. Overall, the alisphenoid is roughly rhomboidal in shape with a vertical diagonal measuring ~60 mm and a horizontal diagonal measuring 70 mm. The alisphenoid–frontal suture appears to be relatively linear and extends anteroventrally for ~45 mm before terminating at the posterodorsal corner of the large orbital fissure. The generally linear alisphenoid–parietal suture slopes posteroventrally and measures ~55 mm. The alisphenoid–squamosal suture is more complex and consists of an irregular anteroventrally sloping segment (measuring ~26 mm) dorsal to the foramen pseudovale and a shorter linear horizontal segment (measuring ~15 mm) anteroventral to the foramen pseudovale (Fig. 7). This latter segment contacts the dorsal portion of the falciform process of the squamosal. The somewhat irregular alisphenoid–pterygoid suture is generally horizontal and extends anteriorly for ~30 mm before terminating at the posteroventral corner of the large orbital fissure. Several small foramina are unevenly distributed along the alisphenoid–parietal suture. As in the basilosaurid archaeocetes *Zygorhiza* and *Dorudon*, the foramen pseudovale does not perforate the alisphenoid externally, but is instead confined to the squamosal (Kellogg, 1936; Uhen, 2004).

Because the temporal walls of many fossil cetacean specimens are incompletely prepared, it is often impossible to interpret the configuration of the alisphenoid and adjacent bones. This is unfortunate given the potential value that clearly defined morphological patterns for these bones would provide to our understanding of cetacean cranial morphogenesis (Ridewood, 1923). The alisphenoid may be especially useful in light of the apparent progressive covering of this bone by the pterygoid during mysticete evolution (our pers. observ.).

Basisphenoid

The basisphenoid is completely covered by the vomer and pterygoid in *Aetiocetus weltoni*. The absence of a clear basisphenoid–basioccipital suture suggests the suture is fused, a condition indicative of developmental maturity. The posterodorsal corner of the basisphenoid is exposed behind the medial pterygoid lamina on the medial border of the peribullar sinus. The sinus is excavated slightly into the basisphenoid.

Dentary

The right and left dentaries are nearly complete. Both, however, are missing the angular process. The coronoid process is very large and lobate as noted by Barnes *et al.* (1995), with a sharp-edged posterior margin (Figs 9, 10). The coronoid process is posteriorly inclined forming an angle of ~60° with the long axis of the ramus. It is not laterally deflected. A conspicuous strut forms the anterolateral corner of the process and defines the anterior border of the masseteric fossa. The straight posterior edge of the coronoid process is inclined posterodorsally and overhangs the neck of the dentary. As the posterior margin descends towards the base of the coronoid process it curves posteriorly to merge with the neck at a point ~35 mm in front of the mandibular condyle (Table 2A). The coronoid process of *Aetiocetus polydentatus* more broadly overhangs the mandibular neck and is more fin-shaped than lobate. In *Morawanocetus yabukii* the coronoid process is rectangular in general outline with a long, straight anterior margin, a blunt dorsal margin and a broadly concave posterior margin. In *Janjucetus* and *Mammalodon* the coronoid process has a broader base and is more triangular, with the posterior margin

Figure 9. *Aetiocetus weltoni*, UCMP 122900, holotype left dentary. A, lateral view; B, medial view.

inclined posteroventrally and not overhanging the neck (Fitzgerald, 2006). In *Eomysticetus* the coronoid process also has a broad base, but is laterally deflected at its dorsal tip. The posterior margin of the coronoid process in this stem edentulous mysticete does not overhang the mandibular neck and instead descends posteroventrally towards the condyle (Sanders & Barnes, 2002). The coronoid processes of basilosaurids are also broad at their bases, but have posterior margins that are nearly vertical to slightly overhanging (Kellogg, 1936; Uhen, 2004).

In *A. weltoni* the neck of the dentary (between the base of the coronoid process and the mandibular condyle) is very short anteroposteriorly (~15mm). In later diverging mysticetes the neck becomes more elongated corresponding to the migration of the coronoid process from a position within the temporal fossa to a position anterior to the temporal fossa and below the orbit. The lateral portion of the neck is the site of insertion of the deep masseter (Schulte, 1916). The mandibular condyle of *A. weltoni* is similar in shape to the condyles of modern odontocetes in being transversely broad dorsally. In posterior aspect the condyle is roughly triangular in shape, with the dorsal surface of the condyle corresponding to the base of the triangle. The lateral margin of the condyle extends ~13 mm beyond the lateral surface of the dentary. In lateral aspect the articular surface of the condyle is broadly convex posteriorly. In medial aspect the margin of the condyle forms the posterior border of the large mandibular foramen (Figs 9, 10). The dorsal margin of this foramen extends anteriorly in a broad arc and descends toward the ventral margin of the dentary. On the left dentary the foramen is 74 mm in length and ~76 mm in maximum height. On the right dentary the anterior margin of the mandibular foramen is complete and indicates that the margin continued ventrally and curved posteriorly toward the broken angular process. It appears that the ventral margin of the mandibular foramen remained slightly above the ventral edge of the dentary and did not merge with it as in some odontocetes. The large size of the mandibular foramen and mandibular canal, coupled with the thin bone on the lateral wall of the dentary adjacent to the foramen, is reminiscent of the condition in basilosaurid archaeocetes and the pan bone of odontocetes.

The horizontal ramus is elongate and narrow transversely and dorsoventrally. There are five distinct mental foramina on the lateral surface positioned 8, 13, 16, 22.6 and 30 cm, respectively, behind the tip of the dentary. These foramina occur 25, 20, 17, 15 and 17 mm, respectively, below the alveolar margin. All foramina are anteroposteriorly elongate and open anteriorly. At the anterior tip of the dentary are two closely appressed circular foramina that open anteri-

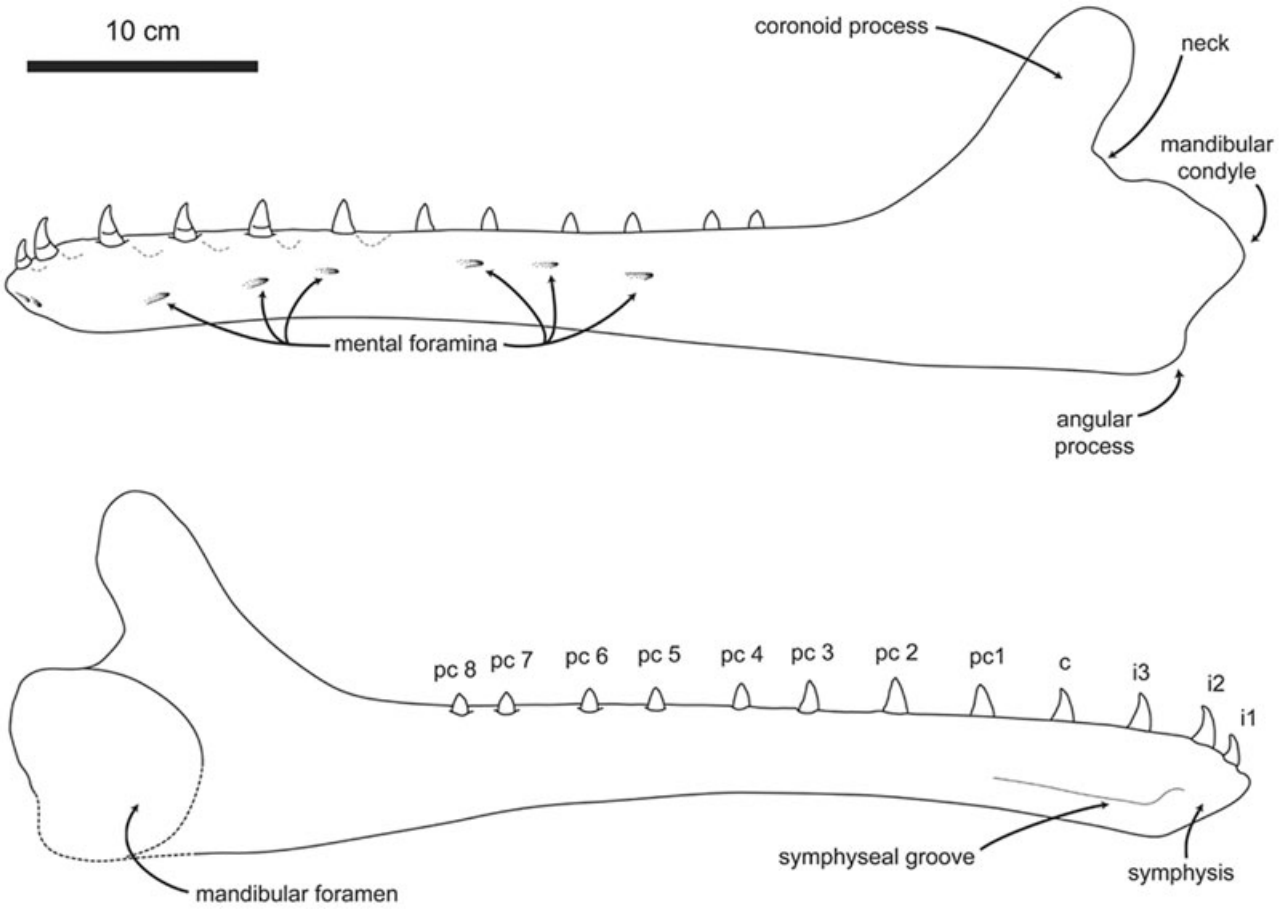

Figure 10. *Aetiocetus weltoni*. A, lateral view of reconstructed left dentary; B, medial view of reconstructed left dentary.

orly. The anteriormost foramen is ~13 mm below the alveolar margin, while the other is approximately 18 mm below the alveolar margin. The dorsomedial edge of the ramus lacks the distinctive gingival foramina present in edentulous mysticetes. This is consistent with the occurrence of an adult dentition in *A. weltoni*, as gingival foramina form in the region of the ossified mandibular alveolar groove during mysticete ontogeny (our pers. observ.).

There are portions of eight postcanine teeth preserved on the left dentary, but only the pc3 crown remains. As noted by Barnes *et al.* (1995) there are alveoli for 12 teeth (eight postcanines), indicating a rudimentary polydont condition. Diastemata along the toothrow are variable in length as follows: i1-2 ~8 mm, i2-3 ~20 mm, i3-c ~21 mm, c-pc1 ~19 mm, pc1-2 ~17 mm, pc2-3 ~25 mm, pc3-4 ~15 mm, pc4-5 ~18 mm, pc5-6 ~16 mm, pc6-7 ~24 mm, and pc7-8 ~5 mm. In occlusal aspect the alveolar margin of the ramus is nearly straight lingually, but distinctly scalloped labially at least to the level of p3. The anterior scalloping is formed by elevated alveolar crests adjacent to each tooth and by embayed embrasure pits or sulci adjacent to each diastema. Strong posteroventrally orientated embrasure pits/sulci occur between i2-3, i3-c, c-pc1 and pc1-2. The orientation of these embrasure pits/sulci suggests that the crowns of the occluding upper teeth were orientated in a similar direction. The best-developed embrasure pits occur between pc1-2 and pc2-3. Posterior to pc3 the labial portion of the alveolar margin in lateral aspect is a continuous linear crest that extends to behind the last postcanine tooth. In occlusal aspect the alveolar region between pc3 and pc8 has indistinct embrasure pits occurring between all preserved alveoli and lingual to the alveolar crest. These embrasure pits received the crowns of the upper dentition. All mandibular teeth appear to be single rooted, although the roots of pc4 and at least pc7 are more anteroposteriorly elongate and appear to represent coalesced anterior and posterior roots. As reported by Fitzgerald (2006) the dentary of *Janjucetus hunderi* has seven, closely spaced, double-rooted postcanine teeth.

In transverse section the labial surface of the horizontal ramus is generally planar, while the lingual margin is convex, at least to the level of pc5. In lateral

aspect the dorsal and ventral margins of the horizontal ramus are roughly parallel. The anterior margin of the dentary is inclined anterodorsally, forming an obtuse angle of approximately 145° with the ventral margin. Posteriorly, the ventral margin is marked by a distinct genial tuberosity.

The anterior tip of the ramus on the lingual side preserves a distinct bony shelf and groove with a curvilinear length of ~40 mm anteroposteriorly (Figs 9, 10). Anterior to the bony shelf and groove is a narrow mandibular symphysis measuring 30 mm in anteroposterior length. The symphyseal surface is smooth and not pitted as in cetaceans with bony/sutural symphyses. (i.e. archaeocetes and odontocetes). Similar and, presumably, homologous features occur on the dentaries of extant mysticetes and are associated with a fibrocartilage skeleton that loosely connects the right and left dentaries (Pivorunas, 1977). This loose mandibular symphysis has been correlated with mandibular kinesis at the intramandibular joint (Lambertsen, 1983) in extant mysticetes and is a feature unique to extant mysticete cetaceans. Its occurrence in *Aetiocetus weltoni* indicates that mandibular kinesis evolved before the loss of teeth in later diverging edentulous mysticetes. Although the lower jaws of *Mammalodon colliveri* and *Janjucetus hunderi* also have non-sutured mandibular symphyses, these toothed mysticetes apparently lack a distinct bony shelf as reported by Fitzgerald (2006).

In dorsal aspect the dentary is broadly convex laterally, a condition shared with all later diverging mysticetes and distinctly different from the laterally concave mandibular configuration of archaeocetes and stem odontocetes. In UCMP 122900 the alveolar margins of the lower and upper jaws align with each other rather precisely during occlusion. This contrasts with the condition in balaenids, neobalaenids and even some balaenopterids in which the lower mandibular arch is conspicuously bowed wider than the rostrum.

Upper dentition

The upper dentition of *Aetiocetus weltoni* is nearly complete and preserved on both the right and the left sides of the rostrum in UCMP 122900. As noted by Barnes *et al.* (1995) there are 11 upper teeth on each side identified as I1-3, C, P1-4 and M1-3. The left dentary was removed from the skull to provide a closer view of the upper dentition. Unfortunately, there has been post-depositional damage to the skull such that the anterior teeth (13-P3) have been distorted slightly with their roots rotated laterally along a longitudinal axis. This is not the case on the right side where these same teeth have a more vertical orientation in the rostrum. Because the right dentary is still articulated with the skull, it preserves the occlusal relationships of the upper and lower dentition, which consists of alternating, interlocking rows of teeth from the rostral tip to M3 (Fig. 4C). The general pattern of the upper dentition consists of procumbent anterior teeth (I1-3 and C, P1) and less procumbent posterior teeth (P2-M3). Most of the procumbency in the anterior dentition is exhibited by the tooth roots, which based on CT imaging are seen to be orientated nearly horizontally within their respective alveoli. The crowns of these same teeth exhibit the greatest amount of curvature. As previously described, broad diastemata occur between all teeth. The left dentition has been prepared and except where noted is the basis for the following descriptions.

The left I1 is nearly complete except for the apex of the crown, which is broken; the right I1 is missing. The I1 crown is only slightly compressed transversely (Table 3) and compared with I2, 3 is nearly conical. Longitudinally, the crown is only slightly curved lingually. On the lingual surface the enamel is marked by fine longitudinal ridges, while the labial enamel is smooth. A distinct crista occurs on the anterolingual corner of the crown. Breakage on the posterior margin of the crown makes it impossible to determine if there was a similar crista in this area. There are no obvious wear facets preserved. The root of the tooth is emergent (i.e. 7–10 mm of the root is exposed outside of the alveolus) and has a larger diameter than the crown (Table 3). Internally (as revealed in CT imaging), the root is orientated anteroposteriorly and extends horizontally ~16 mm into the premaxilla.

The left I2 is a larger tooth and has a more transversely compressed crown than I1 (Table 3). Longitudinally, the crown is slightly curved lingually. In transverse section the lingual surface is nearly planar relative to the more convex labial surface. Although the crown is damaged by fractures, it is relatively complete and can be seen to terminate in a bluntly triangular apex capped by a tiny obliquely orientated (dorsoventral) wear facet. On the lingual surface the enamel is marked by fine longitudinal ridges, while the labial enamel is smooth. A distinct anterior crista is preserved on the crown as in I1. The height of the crown is ~13 mm. As was true for I1 the root of I2 is emergent and exposed for at least 10 mm outside of the alveolus. Internally (as revealed in CT imaging), the root is orientated anteroposteriorly and extends ~14 mm into the premaxilla.

The crown of I3 is unbroken (Table 3) and terminates in a sharply pointed apex that lacks a wear facet. Longitudinally, the crown is more strongly curved lingually than I2. The crown is transversally compressed (planoconvex) with distinct anterior and posterior cristae. The cristae are smooth and not crenulated. On the lingual surface the enamel is

marked by fine longitudinal ridges, while the labial enamel is smooth. The height of the crown is approximately 13 mm. The labial surface of the crown is broadly convex both longitudinally and transversely. The exposed portion of the root is damaged, but like the other incisors extends well outside the alveolus. Internally (as revealed in CT imaging), the root is orientated anteroposteriorly and extends horizontally approximately 7 mm into the premaxilla. The I3 of *Aetiocetus polydentatus* is morphologically very similar.

The upper canine (Fig. 4C) closely resembles I3 in size and shape (Table 3). There are distinct anterior and posterior cristae, a planoconvex cross-section, a sharply pointed apex, a lingual enamel surface with fine longitudinal ridges and a broadly convex (longitudinally and transversely) labial surface with smooth enamel. The height of the crown is approximately 12 mm. In lingual aspect the apex of the crown is placed slightly more posteriorly relative to the more centrally placed apex in I3. This gives the posterior crista a steeper slope than the anterior crista. Internally (as revealed in CT imaging), the root is orientated anteroposteriorly and extends horizontally ~10 mm into the premaxilla. The canine of *Aetiocetus polydentatus* is morphologically very similar.

The P1 closely resembles the canine in all features including the distinct anterior and posterior cristae, planoconvex cross-section, sharply pointed apex with asymmetric lingual profile, lingual enamel with fine longitudinal ridges and a broadly convex (longitudinally and transversely) labial surface with smooth enamel. An abraded wear facet occurs on the anterior crista near the base of the crown. The height of the crown is ~12 mm. Internally (as revealed in CT imaging), the root is orientated more transversely than in the anterior teeth and extends only about 4 mm into the maxilla. The first postcanine of *Aetiocetus polydentatus* is morphologically very similar. Emlong (1966) described an isolated tooth found with USNM 25210 as P1. A tooth catalogued with USNM 25210 and bearing the number 6 appears to be this same tooth. The well-preserved crown closely resembles the P1 of UCMP 122900 with the notable exception of a distinct denticle at the base of the sharp posterior crista and a much weaker denticle at the base of the anterior crista. It is possible that *Aetiocetus weltoni* possessed similar denticles, which have been lost due to wear. The large wear facet on the posterior crista of the UCMP 122900 P1 may have been the site of a posterior denticle. The root is well preserved in the USNM specimen and is relatively short with a posteriorly deflected bulbous termination. There is only a single root.

The crown of P2 has a different morphology from the anterior teeth. Although the left P2 is damaged and slightly corroded, it is clear that the anterior and posterior cristae possess numerous distinct triangular denticles. On the posterior crista are three strong denticles. Anteriorly, the denticles are three in number but are smaller and less distinct. The crown apex is damaged. The lingual surface of the crown is sculpted with a series of fine longitudinal ridges, as noted for the anterior teeth. The labial enamel is smooth. In transverse cross-section the lingual surface is generally planar in contrast to the convex labial surface. The crown was broken at its root at one point and may not have been reattached correctly. As currently positioned the crown is orientated oblique to the sagittal plane and seems to be in an unnatural position. The root is broader than the crown and is not as emergent as in the more anterior teeth. The root is also more bulbous than the roots of preceding teeth. Internally (as revealed in CT imaging), the root is orientated transversely and extends only about 4 mm into the maxilla. There appears to have only been a single root. The P2 assigned by Emlong (1966) to *A. cotylalveus* is well preserved and has a lingually bowed crown with three strong denticles on the sharp posterior crista and two weaker denticles at the base of the anterior crista. The enamel on the lingual surface has 12–14 fine longitudinal ridges, while the labial enamel is smooth. The root is single-rooted. The second postcanine tooth of *A. polydentatus* has smooth anterior and posterior cristae and lacks the distinct denticles noted in *A. weltoni* and *A. cotylalveus*.

The crown of P3 is poorly preserved, with all surfaces exhibiting some degree of damage. This includes the anterior and posterior margins, which do not preserve the denticles seen on P2. It is likely that denticles occurred on these teeth, but this cannot be confirmed. The crown of P3 was also broken at its root and seems to have been reattached in an unnatural position. The root of P3 is quite bulbous and is distinctly broader than the crown. Internally (as revealed in CT imaging), the root is orientated transversely and extends only about 4 mm into the maxilla. There is only a single root. The isolated tooth assigned by Emlong (1966) to this tooth position is better preserved and characterized by a series of four small worn denticles arranged along the anterior crista. A large wear facet on the ventral edge of the posterior crista removed any trace of denticles that may have been positioned here. The crown is planoconvex in cross-section, the lingual enamel is finely ridged and the labial enamel is smooth. Emlong (1966) describes a slight longitudinal median groove on both the internal and the external sides of the root that he interprets as evidence for two coalesced roots. The third postcanine of *A. polydentatus* has a crown of similar size to the P3 of *A. cotylalveus*, but has only

two denticles, one each positioned near the base of the anterior and posterior cristae.

The crown of the left P4 of *A. weltoni* is damaged to the point that little is left to describe. The isolated tooth of *A. cotylalveus* assigned by Emlong (1966) to P4 has a crown with four small denticles arranged along the anterior crista and a large wear facet along the posterior crista. In transverse section both the labial and the lingual surfaces are convex in contrast to the planoconvex cross-sections observed in I1-P3. The labial enamel is still smooth, but the lingual enamel consists of fine, longitudinal, wavy ridges. According to Emlong (1966) the root has a longitudinal median groove suggesting two coalesced roots. The fourth postcanine tooth of *A. polydentatus* has a crown with two small denticles near the base of the anterior crista and three stronger denticles on the posterior crista. In lingual aspect the crown is nearly symmetrical with the posterior margin being only slightly steeper than the anterior margin. In transverse section both the labial and the lingual surfaces are convex.

The crown of the left M1 of *A. weltoni* is also damaged to the point that little is left to describe. The isolated tooth of *A. cotylalveus* assigned by Emlong (1966) to M1 has a crown with three small denticles arranged along the posterior crista and a small wear facet along the anterior crista. A single tiny denticle remains at the base of the anterior crista. In transverse section both the labial and the lingual surfaces are convex. The labial enamel is still smooth, but the lingual enamel consists of fine wavy (not linear) longitudinal ridges. According to Emlong (1966) the root condition is still single-rooted with no longitudinal median groove. The fifth postcanine tooth of *A. polydentatus* has a crown with three small denticles near the base of the anterior crista and two stronger denticles on the posterior crista. The crown is symmetrical in lingual aspect and in transverse section both the labial and the lingual surfaces are convex. As in other species of *Aetiocetus*, the labial enamel is smooth, while the lingual enamel has fine, longitudinal ridges.

The crown of the left M2 in UCMP 122900 has a symmetrical triangular shape in lateral aspect and somewhat resembles the teeth of squalodontid odontocetes (Kellogg, 1923). The posterior margin of the crown is slightly damaged, but preserves one accessory denticle and the broken base of another denticle. The apex of the crown (paracone) is sharply pointed and the anterior margin is slightly damaged but does not appear to have possessed any denticles. Overall, the crown is strongly convex lingually and weakly convex labially. Although abraded, the enamel on the lingual side of the crown bears faint remnants of fine longitudinal ridges near the cingulum. The anterolingual portion of the crown is convex both transversely and longitudinally, while the posterolingual portion is more sharply angled at its juncture with the posterior crista. The root of M2 is damaged. The sixth postcanine tooth of *A. polydentatus* is too damaged for comparisons to be made.

M3 resembles M2 in its overall triangular and symmetrical shape, but is slightly smaller in size (Table 3). The posterior margin of the crown preserves the worn bases of two closely appressed denticles. The crown apex (paracone) is sharply pointed and the anterior margin of the crown preserves a broad wear facet that has obliterated any trace of denticles that may have been present. The lingual surface of the crown is generally convex transversely with weakly developed wavy longitudinal ridges adjacent to the cingulum. The labial margin is more broadly convex both transversely and longitudinally and has smooth enamel. The root of this tooth is not well preserved. The seventh postcanine tooth of *A. polydentatus* has a crown with three small denticles evenly spaced along the anterior and posterior cristae. The crown is symmetrical in lingual aspect and in transverse section and both the labial and the lingual surfaces are convex. The crown of the eighth postcanine tooth of *A. polydentatus* preserves four strong denticles on the anterior crista and a large wear facet on the posterior margin. Like PC7 both the labial and the lingual surfaces of the crown are convex. The crown of the ninth postcanine tooth preserves only a single denticle on the anterior margin, the remainder of which is characterized by a large wear facet. A similar wear facet has removed all traces of denticles from the posterior margin of the crown.

Lower dentition

Portions of the lower dentition are preserved in both dentaries (Figs 4C, 9; Table 2B). As noted by Barnes *et al.* (1995) there are 12 lower teeth on each side identified as i1-3, c, pc1-8. The left dentary has been removed from the skull making it possible to examine the left toothrow closely. Unfortunately, there are broken crowns and missing teeth for most tooth positions. The right dentary is still articulated with the skull and, although most of the right dentition is preserved except for i1, the teeth posterior to pc1 are hidden from view by the overriding maxilla. The general pattern of the lower dentition consists of procumbent anterior teeth (i1-3, c and pc1) and less procumbent posterior teeth (pc2-pc8). All teeth are separated by distinct diastemata, although the length of diastemata decreases from front to back.

The crown of the left i1 is broken and only the root is preserved. The root is damaged but appears to have been circular in cross-section.

The left i2 preserves a short segment of the base of the crown. Very fine longitudinal enamel ridges are

preserved only on the lingual side of the crown, which has a smaller diameter than the more bulbous root. The labial surface of the right i2 is nearly complete and is broadly convex transversely (Table 5). The crown terminates in a sharply pointed apex that is bordered anteriorly by a sharp crista and posteriorly by a more delicate crista. The crown height is approximately 15 mm. As preserved, the right tooth is almost out of its alveolus.

The crown of the left i3 is broken while that on the right side is complete. The crown is broadly convex transversely and longitudinally on the labial side. The enamel surface on the labial side is generally smooth, although there are several broad longitudinal ridges that converge toward the apex. The diameter of the crown is greater than that of i1, but is still smaller than the diameter of the more bulbous root (Table 5). Although closely appressed to the lateral margin of the maxilla, it appears that the crown of the right i3 had anterior and posterior cristae. This suggests that the lingual margin was probably flattened and not convex.

The canine is absent from the left dentary and is incompletely preserved in the right dentary. Unfortunately, the apex of the crown is broken. The labial surface is broadly convex transversely with smooth enamel and broad longitudinal ridges similar to those noted on i3. The ventral 5 mm of the anterior crista is clearly evident on the crown. The condition of the posterior margin of the crown, however, is obscured due to its proximity to the maxilla. The diameter of the root is slightly greater than that of the crown.

Only the root of the left pc1 is preserved in the dentary while the right pc1 is slightly more complete with at least the base of the crown preserved. A clean break reveals distinct concentric growth lines in the centre of the tooth near the base of the crown. The base of the crown is swollen. The root is ovoid in cross-section with the longest dimension orientated anteroposteriorly. The root is broader and more bulbous than the base of the crown.

The left pc2 is not preserved and the right pc2 is incomplete. The apex of the crown protrudes into the overlying maxilla and has been broken by post-depositional compaction. The anterior margin of the crown preserves two distinct triangular denticles similar to those noted on the crown of P2. The posterior margin is broken. The root is ovoid in cross-section with the longest dimension orientated anteroposteriorly. The root is broader and more bulbous than the base of the crown.

The tooth preserved in the alveolus for the left pc3 is nearly complete although twisted 180° around its long axis. Overall the crown is narrowly triangular in lateral aspect terminating in a sharply pointed apex. The enamel on the labial surface is generally smooth, although there are two broad longitudinal ridges converging apically. The posterolabial corner of the crown preserves a relatively large wear facet while the anterolabial corner of the crown is unworn. The distinct anterior crista is smooth and lacks any evidence of the denticles noted on p2. The enamel on the lingual surface of the crown is roughened and characterized by numerous fine longitudinal ridges. The right pc3 is probably complete, but because of the tight occlusion of the upper and lower jaws much of the tooth is obscured. The dorsal surface of the maxilla immediately above the right pc3 is slightly elevated probably due to protrusion of the pc3 crown into the ventral surface of the maxilla. As preserved and prepared the labial portions of the crown of pc3 are partially visible. The enamel is smooth and the anterior margin of the tooth bears at least two sharply pointed denticles as for pc2. The diameter of the crown appears to be nearly equal to that of the ovoid root (Table 4).

The crown of the left pc4 is broken and only the root is preserved. The root is apparently ovoid with a distinct longitudinal sulcus on the labial side suggesting fusion of anterior and posterior roots. The diameter of the crown is distinctly smaller than that of the root. Although the right pc4 is probably preserved in the skull, it has not been prepared and cannot be described. The same can be said for the molar series on the right side.

On the left side there are no crowns preserved for the posterior teeth and only the roots of pc6 and pc7. The root of pc7 is bilobed with central sulci labially and lingually suggesting fusion of anterior and posterior roots. The open alveolus for the last postcanine tooth is shallow and ovoid. On the right side a portion of the crown of pc7 is partially exposed between the closely appressed crowns of the adjacent teeth. Overall the crown is symmetrical and broadly triangular in lateral aspect terminating in a sharply pointed protoconid apex. The enamel on the labial surface is smooth and the anterior margin of the crown preserves three distinct accessory denticles. The denticle nearest the base of the crown is the smallest and shows apical wear.

DISCUSSION

Comparisons with other aetiocetids

Barnes *et al.* (1995) offered three characters to distinguish *Aetiocetus weltoni* from *A. cotylalveus*, including: rostral bones extending posteriorly to a point between the posterior margins of the supraorbital process of the frontals, squamosal fossa more anteroposteriorly elongate, and dental count 11/12. One of these features, the dental count, as noted by them, is

Table 5. Character–taxon matrix showing distribution of cranial and dental character states among selected toothed mysticetes and related taxa

	Character									
	10		20		30		40		50	
Taxon	12345	67890	12345	67890	12345	67890	12345	67890	12345	6
Dorudon	00000	00000	00000	00000	00000	00000	00000	00000	00000	0
Zygorhiza	00000	00000	00000	00000	00000	00000	00100	01000	00000	0
Agorophius	00003	02120	10?0?	00?01	0?0??	0?221	00111	?1001	00000	0
Tasmacetus	10203	03120	10100	00112	22000	02320	03002	21000	00000	1
Mammalodon	200?1	1002?	?????	?0??1	11?1?	100?1	01010	??02?	00000	?
Janjucetus	20021	10100	101??	011?1	?1010	10010	01010	?002?	0?001	1
Aetiocetus tomitai	?00??	1?121	1????	?10??	?????	??2?1	0?100	102??	0000?	2
Aetiocetus weltoni	20011	22011	11210	11012	10101	21211	02100	11121	00001	2
Aetiocetus cotylvaeus	20011	20121	11210	11012	10101	??211	02100	11121	00001	2
Aetiocetus polydentatus	20012	10011	11210	?1012	20101	21211	02110	11221	00001	2
Morawanocetus	200??	10121	1???0	10111	110?1	?1011	0110?	111??	00001	1
Chonecetus goedertorum	20021	1012?	01210	11012	???11	21211	0?100	10210	00001	2
Eomysticetus	01000	11000	??00?	?000?	????1	202?1	0?010	2?2??	11111	2
Crown Mysticetes	a1/21/20/3a	0/1b120	10001/2	1000?	????1/2	23b11	1?00/10/1	20/1110/1	11111	b

Character states scored 0 represent ancestral state, 1–3 represent derived states. a = 0/2/3, b = 0/1/2. Missing data are scored as ?.

probably the same in both species (the dentary is unknown for *A. cotylalveus*). The length of the squamosal fossa was not quantified by Barnes *et al.* (1995) and when compared by us for the two taxa seems to be a subjective distinction. Rostral bones that extend further posteriorly in *A. weltoni* are indicative of the greater degree of telescoping of the skull. We considered the possibility that this difference was due to individual variation within a single species. To test this we made a limited comparison of the region of rostral–cranial interdigitation in several specimens of a modern mysticete, *Balaenoptera acutorostrata* (minke whale), and in an aetiocetid, *Chonecetus goedertorum*, known from two skulls. In neither case was there significant variation in the extension of the rostral bones. This result supports the recognition of *Aetiocetus weltoni* and *A. cotylalveus* as distinct species, as does the narrower transverse intertemporal width, more robust zygomatic process of the squamosal and less lobate anterior parietal wings of *A. weltoni*.

Aetiocetus polydentatus differs most strikingly from *A weltoni* and *A. cotylalveus* in its greater degree of polydonty and its longer and broader nasals (Barnes *et al.*, 1995). Ichishima (2005) suggested that *A. polydentatus* was not a member of *Aetiocetus* noting the following character states: (1) parasagittal crests on the parietals in the intertemporal region; (2) lateral margin of maxilla bending ventrally; and (3) relatively distinct temporal crests on posterior margin of supraoccipital process of frontal. Fitzgerald (2006) agreed that *Aetiocetus* was probably paraphyletic and that *A. polydentatus* was a more derived species. In support of this hypothesis, Fitzgerald (2006: supplement) noted the following character states: (4) ascending process of maxilla terminates slightly posterior to antorbital notch, at a point level with the anterior third (anteroposteriorly) of the supraorbital process of frontal; (5) anteroposteriorly foreshortened supraorbital process of frontal; (6) poorly developed concavity in lateral margin of supraorbital process such that the orbit opens laterally but not anterolaterally and dorsolaterally; and (7) elongated intertemporal region with well-developed sagittal crest. In evaluating these seven purported distinguishing characters we made the following conclusions: (1) the parasagittal crests in the intertemporal region are an autapomorphy of *A. polydentatus*; (2) the ventral deflection of the lateral margin of the maxilla is probably a diagenetic distortion; (3) the strong temporal crests are an extension of the distinct parasagittal crests; (4) the apparent anterior termination of the ascending process of the maxilla is a preservational artefact; (5) the apparent anteroposteriorly shortened supraorbital process of the frontal is also a preservational artefact; (6) although the orbital rim is less embayed, poor preservation may be contributing to the effect; and (7) the intertemporal region is no more elongate than in other species of *Aetiocetus*. We conclude from this review that although *A. polydentatus* does possess distinct features, when viewed in a phylogenetic context (see below) these features are not sufficient to remove this taxon from the *Aetiocetus* clade.

Aetiocetids as transitional taxa

The toothed aetiocetids from Oligocene rocks of the North Pacific can play a key role in interpretations of cetacean evolution because they are transitional in grade between archaeocetes and extant edentulous mysticetes. In turn, *Aetiocetus weltoni* has important implications for mysticete phylogeny and for refining the definition and diagnosis of Aetiocetidae. The skull and dentary of *A. weltoni* preserve a number of morphological features that underline this transitional position of aetiocetids. The anterior placement of the external nares is reminiscent of dorudontine archaeocetes, as are the elongate nasals, dorsally placed supraorbital frontal processes, distinct intertemporal parietal exposure, flat palate with teeth, rigid rostrum, large and lobate coronoid process of dentary positioned in temporal fossa, and large mandibular fossa. Except for the flat, toothed palate and relatively rigid rostrum, all of these plesiomorphic features also occur to some extent in the stem edentulous mysticete *Eomysticetus whitmorei*. However, both *Eomysticetus* and *Aetiocetus* possess important features unique to mysticetes, including an edentulous and transversely expanded infraorbital maxillary plate, robust basioccipital crests, outwardly bowed dentary and mandibular symphyseal groove. In this light, the retention of an adult heterodont dentition in species of *Aetiocetus* emphasizes the mosaic nature of this group of toothed mysticetes.

It seems clear that mysticete evolution has at its core involved an expansion of the oral cavity volume. Among extant mysticetes this has been accomplished in a variety of ways. Balaenopterids have increased oral volume through broadening of the rostrum and a functional expansion of the ventral portion of the oral cavity via a ventral throat pouch (Pivorunas, 1979; Lambertsen, 1983). Balaenids have increased oral volume through dorsal arching of the rostrum and elongation of the baleen plates (Pivorunas, 1979). *Eschrichtius* has increased oral volume in a somewhat similar fashion with functional expansion of the dorsal portion of the oral cavity (i.e. rostral arching), but also utilizes a minor degree of ventral throat expansion coupled with oral suction (Pivorunas, 1979).

All groups rely on cranial and mandibular kinesis to accommodate the increased oral cavity volume.

Cranial kinesis involves unfused and loosely joined intra- and inter-rostral articulations (e.g. lack of fusion between maxilla and premaxilla, between maxilla and vomer, between maxilla and frontal, and between premaxilla and frontal) (Berta *et al.*, 2006). In contrast, rostral sutures in archaeocetes and odontocetes are distinctly fused. Published accounts of mysticete cranial kinesis, surprisingly, are largely confined to brief discussions of the loose nature of mysticete rostral sutures (Miller, 1923; Kellogg, 1928). Mandibular kinesis involves a loose mandibular symphysis that allows a surprising degree of independent movement of the right and left dentaries at the symphysis (Lambertsen, Ulrich & Straley, 1995). In both cases the kinetic anatomical conditions decrease torque-related strain during bulk feeding. Species of *Aetiocetus* possess some of the features correlated with mandibular kinesis, but lack the features associated with rostral kinesis (i.e. they retain the archaeocete condition of a rigid rostrum).

Aetiocetid dentition

Morphologically, the teeth of *Aetiocetus weltoni* are markedly similar to those of *A. cotylalveus* and *A. polydentatus* in size, enamel texture and overall shape, although not tooth count. All teeth have a smooth enamel surface on the lateral (labial) side of the crown, while the medial (lingual) side of the crown has a roughened surface texture composed of fine, generally longitudinal enamel ridges. Barnes *et al.* (1995) considered species of *Aetiocetus* to be homodont; however, the dentitions are in fact weakly heterodont. In all known species the crown of I1 is roughly conical, while those of I2, 3 are transversely compressed, laterally and posteriorly curved, and have sharp anterior and posterior cristae. The upper canine and first postcanine closely resemble I3 with the exception that they are less curved. In *A. weltoni* the P2 crown is planoconvex in transverse cross-section (planar lingually and convex labially) and has three small anterior and three posterior accessory denticles on either side of the sharply pointed principal cusp. In *A. polydentatus* numerous accessory denticles do not occur until the fourth postcanine tooth; the second postcanine lacks accessory denticles and the third postcanine has only a single denticle anteriorly and posteriorly. In this taxon the crown of the second and third postcanines are planoconvex in transverse section, while that of the fourth postcanine is convex on both sides. In *A. weltoni* this change from planoconvex to convex–convex cross-sections probably occurs between P3, 4. In the latter taxon the crowns of M2, 3 are different from those of all preceding teeth in being roughly triangular in lateral profile with sharply pointed principal cusps (paracones) flanked posteriorly by two accessory denticles. The anterior cristae of these teeth lack denticles. Thus, the dentition of *A. weltoni* consists of anterior caniniform teeth (I1-3, C, P1), central equally denticulate teeth (P2-4), and posterior asymmetrically denticulate teeth. An isolated right M2? associated with the holotype of *Morowanocetus yabukii* (AMP 1) preserves a very different crown morphology with both roughened labial and lingual enamel surfaces consisting of strong irregular ridges converging on the apex, a low paracone, and the worn bases of two anterior and three posterior accessory denticles. The crown is larger than in any teeth of *Aetiocetus* spp. and measures 16.3 mm in anteroposterior length, 7.96 mm in transverse width and 11.05 mm in crown height. The accessory denticles of *M. yabukii* are large and nearly the same size as the paracone. The dentition of *Janjucetus hunderi* is also distinctly different from *Aetiocetus* spp. and consists of heavily ridged enamel on both the labial and the lingual surfaces of the crowns, large multiple accessory denticles on the posterior edge of P2-M2 and double rooted postcanines (Fitzgerald, 2006). In *Llanocetus* only the morphology of the lower postcanine teeth has been described (Mitchell, 1989), but these teeth are also quite different, with very roughened labial and lingual enamel surfaces, a relatively small principal cusp (protoconid), and numerous relatively large and palmate anterior and posterior accessory denticles.

The presence or absence of baleen in aetiocetids

The mosaic condition of aetiocetids with their mixture of primitive dorudontine archaeocete characters, stem mysticete characters and adult dentition begs the question: 'Did species of *Aetiocetus* possess baleen?' Previous workers think not. Barnes *et al.* (1995) were equivocal in their treatment of this matter, although their stated dichotomy between aetiocetids and 'baleen-bearing mysticetes' implies that they felt that aetiocetids lacked baleen. In a later report, Sanders & Barnes (2002) stated, 'It seems most probable that the Aetiocetidae and the Mammalodontidae are side branches of Mysticeti in which baleen was never developed, the retention of teeth into adulthood perhaps being a paedomorphic character that became firmly entrenched.' In a more recent report, Geisler & Sanders (2003) suggest that baleen was absent in aetiocetids because these taxa lacked large vascular foramina on the palate. This latter point is discussed below.

Without preservation of actual baleen or impressions of baleen found with fossil aetiocetids this question cannot be unequivocally answered. The vascular system necessary to nourish baleen, however, does

leave bony landmarks on the palate of modern mysticetes. The clearest of these landmarks are the lateral foramina and associated sulci of the palate. As described recently by Deméré *et al.* (2008), the series of delicate lateral palatal foramina and sulci of *Aetiocetus weltoni* are hypothesized as the landmarks of a palatal vascular system for rudimentary baleen. These authors contend that these lateral palatal foramina are homologous with the prominent baleen nutrient foramina in edentulous mysticetes.

The palates of extant mysticetes are marked by numerous foramina and associated sulci. A general distinction can be made between foramina positioned near and parallel to the midline and foramina more laterally placed and often radially arranged. The latter foramina provide passage of the rich blood supply to the baleen racks (Walmsley, 1938). In fetal specimens of modern mysticetes the lateral foramina have not yet formed and instead there is a distinct open alveolar groove running along the lateral margin of the flat palate (Ridewood, 1923). Embryologically, this alveolar groove is the site of the developing temporary dentition, which passes through the bud, cap and bell stages of development before degradation and resorption of the deciduous tooth buds begins (Karlsen, 1962; Ishikawa & Amasaki, 1995; Ishikawa *et al.*, 1999). Dermal papillae of the rudimentary baleen plates begin to develop coincident with tooth bud degradation. At the same time the open alveolar groove starts to fill with bone until finally the distinct lateral nutrient foramina begin to form. This progressive ossification also involves a widening of the palatal region above the developing baleen racks.

Given the close association between tooth and baleen development observed in modern mysticetes it is plausible that we are seeing an ancient ontogeny expressed in *Aetiocetus*. As described by Deméré *et al.* (2008), *Aetiocetus weltoni* possessed both baleen and a functional adult dentition and thus indicates that the evolution of mysticete bulk feeding involved a step-wise process from the ancestral condition of teeth only, through an intermediate condition with both teeth and baleen, to the derived condition with baleen only. The form of this early baleen system of *Aetiocetus* is currently unknown, but perhaps consisted of small bundles of keratinized tubules similar to those occurring at the front and rear of the main baleen racks of modern balaenopterids. In *Aetiocetus* such bundles could have formed a rudimentary brush-like filter between the widely spaced teeth of the upper dentition. It is tempting to speculate that even *Llanocetus* had rudimentary baleen, a hypothesis supported by the report of abundant fine grooves around the tooth alveoli on the palate of this southern hemisphere Palaeogene toothed mysticete (Fordyce, 2003).

Feeding apparatus of aetiocetids

The long rostrum and dentaries, the relatively posterior position of the coronoid process on the dentary, the large size of the coronoid process, the location of the coronoid process within the relatively large temporal fossa and restricted origins of the temporal musculature (i.e. essential absence of the temporal muscles from the supraorbital processes of the frontals) suggest that *A. weltoni* was capable of a snapping style jaw adduction, not unlike that proposed for dorudontine archaeocetes (Uhen, 2004) and stem odontocetes (Fordyce, 2002). This is the primitive condition and suggests that *A. weltoni* did not utilize sustained mandibular abduction during filter feeding as in extant balaenids. These cranial and mandibular features also seem counter to those necessary for the extreme depression of the dentary (Delta rotation) and lateral deflection at the tempormandibular joint (Omega rotation) reported in extant balaenopterids (Lambertsen *et al.*, 1995). It is clear that species of *Aetiocetus* were capable of kinesis at the mandibular symphysis (Alpha rotation), which was probably deployed during expulsion of water from the enlarged oral cavity as the mouth was closing. Assuming the presence of a rudimentary baleen apparatus, the water flowing out of the closing mouth passed through the baleen trapping concentrations of schooling prey species. In contrast, single prey were probably captured by the functional adult dentition in the primitive pierce feeding fashion employed by dorudontine archaeocetes. In both cases the size of prey species was limited by the spacing between baleen elements and/or teeth.

Questions of feeding strategy in toothed mysticetes have recently been summarized by Fitzgerald (2006) who concludes that the crabeater seal analogue model of tooth-aided filter feeding in these taxa is probably incorrect. He cites the lack of closely appressed teeth with elaborately denticulated postcanine crowns as an obstacle to a filter-feeding interpretation. However, this argument assumes that the prey species are small and near the size of krill. The problem with this approach is that it assumes filter feeding as a strategy and small size as a prey choice. Filter feeding at its core can be thought of as bulk feeding. Prey size is not part of this basic definition. In fact, contrary to conventional wisdom, not all living baleen whales eat krill. Given the range of prey type and size seen in extant mysticetes, there is no reason to assume *a priori* that species of *Aetiocetus* fed on small prey (i.e. krill)? Their bulk feeding behaviour could have focused on larger prey (e.g. schooling sardines or squid). The principal requirement for bulk feeding is enlargement of the oral cavity and aetiocetids had larger mouths than archaeocetes, a feature that can be viewed as an

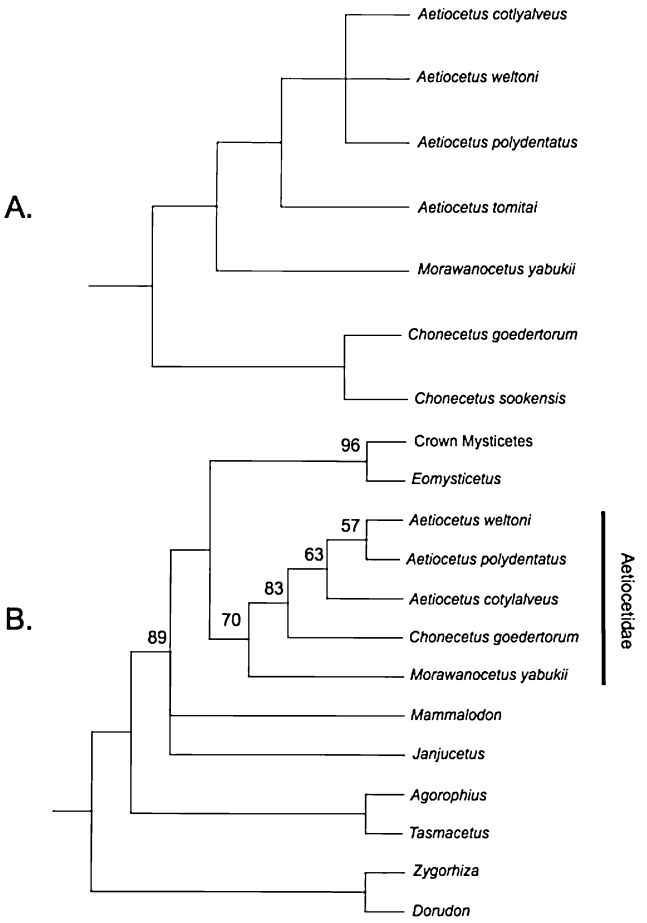

Figure 11. Phylogenetic hypotheses of aetiocetid relationships. A, previous study based on Barnes *et al.* (1995); B, this study.

adaptation for bulk feeding. In turn, their more widely spaced and less lobate teeth could still be functional as a coarse sieve in filter feeding. The evolutionary development of baleen in aetiocetids in combination with their dentition would serve to expand the prey choices for these transitional mysticetes.

PHYLOGENETIC RELATIONSHIPS OF *AETIOCETUS*

Emlong (1966) in his original description of *Aetiocetus cotylalveus* made comparisons with basal odontocetes (*Agorophius* and *Archaedelphis*) and archaeocetes (*Patriocetus*, *Microzeuglodon* and *Agriocetus*). He concluded that 'the degree and trend of telescoping are more suggestive of the Mysticeti' although the presence of teeth prompted Emlong to exclude *Aetiocetus* from inclusion within this lineage. The presence of several purported archaeocete features (e.g. narrow and very elongate intertemporal region and a functional adult dentition) supported its assignment to this group.

The phylogenetic relationships of *Aetiocetus* to other aetiocetids has been discussed by Barnes *et al.* (1995) who recognized *Chonecetus* as the most basal aetiocetid with *Aetiocetus* positioned as a later diverging taxon sharing a sister group relationship with *Morawanocetus* (Fig. 11). Barnes *et al.* (1995) were unable to resolve relationships among species of *Aetiocetus*. Our hypothesis for the position of aetiocetids and related species is shown in Figure 11.

Previous studies have identified different suites of characters to diagnose the Aetiocetidae (characters from prior studies are numbered sequentially below to facilitate discussion). Barnes *et al.* (1995) originally identified five characters: (1) protuberance on premaxilla at anterolateral corner of nasals; (2) multiple maxillary foramina; (3) groove in dentary for symphyseal ligament; (4) zygomatic process long and slender; and (5) squamosal fossa short. This list was reduced to characters 1 and 3 by Sanders & Barnes (2002), who considered only two characters as unique to aetiocetids: (6) intertemporal region shortened anteroposteriorly and widened transversely; and (7) elongate

notch present in posterior border of palatine at posterior edge of palate. Geisler & Sanders (2003) identified the following three aetiocetid synapomorphies: (8) three or more infraorbital facial foramina; (9) premaxillae adjacent to and at posterior edge of the nasal opening overhang the maxillae; and (10) cross-section through intertemporal region, including parietals ovoid but sagittal crest absent. We re-evaluated these characters and placed them into one or more of three categories: (1) characters we use in the present analysis; (2) characters with an incorrect reported taxonomic distribution; and (3) characters minimally described (e.g. lack of quantification). Our reallocation of these characters is summarized below. We found one character to require no amendment and we used it in the present study (#7). We found that six characters have an incorrect distribution reported (#1, 2, 3, 4, 8, 10). Finally, into the third category, we assigned two characters (#5, 6). Character #9 is equivalent to #1 as both are describing the relative position of the premaxilla and maxilla adjacent to the external narial opening.

In our study we evaluated 46 craniodental characters (22 binary and 24 multistate; Table 5). All characters and character-state transformations were unweighted and all multistate characters were unordered. We considered 11 ingroup taxa: six aetiocetids (*Aetiocetus tomitai*, *A. weltoni*, *A. cotylalveus*, *A. polydentatus*, *Morawanocetus yabukii* and *Chonecetus goedertorum*), two other toothed mysticetes (*Janjucetus hunderi*, *Mammalodon colliveri*), the basal edentulous mysticete *Eomysticetus whitmorei*, and all crown mysticetes (i.e. Balaenidae, Balaenopteridae, Eschrichtiidae and Neobalaenidae). We excluded the poorly preserved *A. tomitai* from later runs of the data as its inclusion failed to resolve relationships among other species of *Aetiocetus*. For outgroup taxa we employed the following: two dorudontine archaeocetes, *Dorudon atrox* and *Zygorhiza kochii*, and two basal odontocetes, the extinct *Agorophius* sp. (ChM 5852) and the extant ziphiid *Tasmacetus shepardi*. We used the branch and bound search option of PAUP*vb10 (Swofford, 2001) with a maximum parsimony optimality criterion. All multistate characters were treated as unordered. Character optimizations explored both ACCTRAN (which favours reversals over parallelisms) and DELTRAN (which favours parallelisms over reversals) although our preferred hypothesis of character evolution followed the DELTRAN optimization. Our rationale for this decision is that for characters scored as unknown (?) for some taxa (e.g. *Mammalodon*) using ACCTRAN would result in hypothesizing the presence of certain character states in taxa in which there is no evidence that these states were ever present. The cladistic analysis produced one most parsimonious tree with a tree length of 106 steps and a rescaled consistency index of 0.4746 (Fig. 11). Based on our analysis we recognize the monophyletic groups/taxa discussed below. Bootstrap percentages based on 1000 replicates were calculated and are shown in Figure 11. Mysticete monophyly was reasonably well supported (68%) as was monophyly of the edentulous mysticetes (96%). Mysticeti monophyly was supported by two unequivocal characters: mandibular symphysis not sutured (26) and anterior and postcanine teeth moderately heterodont, weakly heterodont, or absent (32). A clade containing *Mammalodon* and later diverging mysticetes is diagnosed by two unequivocal synapomorphies: descending process developed as an infraorbital plate (29; transformation from 2 to 1) and lateral margins of maxillae thin (45). *Mammalodon* is distinguished from other mysticetes by one equivocal character: intertemporal region narrow (8; reversal 1 to 0).

AETIOCETIDAE
(*AETIOCETUS* + *CHONECETUS* + *MORAWANOCETUS*)

This monophyletic group is diagnosed by three unequivocal synapomorphies (Fig. 11): zygomatic process of squamosal expanded near its anterior margin and at its posterior end but narrow in the middle (10), coronoid process well developed with concave posterior margin (27), and short overlap of jugal with squamosal (36). Three equivocal synapomorphies are potentially diagnostic of this clade: posterior sinus poorly developed or absent (19), preglenoid portion of squamosal with short anteriorly convex subtemporal crest extending into temporal fossa (33) and lambdoidal crests flush with temporal wall (34; reversal from 1 to 0). This clade is well supported (bootstrap value 70%). *Morawanocetus*, identified as the most basal aetiocetid, is diagnosed by two equivocal characters: long basicranial width (18) and posterior process of premaxilla contacting the frontal (46; transformation from 2 to 1). *Chonecetus* and *Aetiocetus* spp. are united as sister taxa by two unequivocal characters: lacrimal exposed dorsally (12) and posterior margin of palatine with notch (14). Four additional equivocal characters are potentially diagnostic of this clade: palate window exposing vomer present and formed by maxilla and premaxilla (13; transformation from 0 to 2), squamosal fossa with second fossa developed (17), posterior teeth single rooted (20; transformation from 1 to 2, and posteriormost edge of nasals located on the posterior half of the supraorbital process of frontal (28; transformation from 0 to 2). *Chonecetus* is diagnosed by five equivocal synapomorphies: triangular anterior extension of parietal–frontal suture (4), zygomatic process of squamosal does not reach level of supraorbital process of frontal (11; reversal from 1 to 0), anterior position of posterior end of ascending process of maxilla relative

to posterior extremity of nasal (37; reversal from 1 to 0), posterior position of posterior extension of premaxillae relative to posterior extremity of maxillae (38; transformation from 1 to 2, and oblique groove on anterolateral face of zygomatic process of maxilla present but low (39; transformation from 2 to 1).

AETIOCETUS

This clade is diagnosed by two unequivocal synapomorphies: anterior and posterior denticles on posterior upper teeth three or fewer, small and simple (23) and anterior and postcanine teeth weakly heterodont (32; transformation from 1 to 2). An additional four characters are potentially diagnostic of this clade: triangular anterior extension of parietal–frontal suture (4), vertical enamel ridges only on lingual surface of postcanine teeth (22; reversal from 1 to 0), teeth with wide diastemata (24; reversal from 1 to 0) and rostral width at antorbital notch (base) relative to occipital condyle width > 170% (40). This clade is not well supported (bootstrap value 58%). *Aetiocetus cotylalveus* is identified as the most basal *Aetiocetus* species and is diagnosed by a single equivocal character: supraorbital process of frontal with deeply concave orbital rim (6). The later diverging species of *Aetiocetus* (*A. weltoni* + *A. polydentatus*) are diagnosed by two equivocal synapomorphies: intertemporal region narrow (8; reversal from 1 to 0) and sagittal crest reduced (9). *Aetiocetus weltoni* is diagnosed by two equivocal characters: deeply concave orbital rim (6) and posteriormost edge of ascending process of maxilla terminates at the posterior border of the supraorbital process of frontal (7; transformation from 0 to 2). *Aetiocetus polydentatus* is diagnosed by four equivocal characters: broad nasals (5; transformation from 1 to 2), a high tooth count (21; transformation from 1 to 2), lambdoidal crests overhanging temporal wall (34) and posterior extension of premaxilla posterior to posterior extremity of maxilla (38; transformation from 2 to 1).

CONCLUSIONS

Aetiocetids represent an important group of toothed mysticetes that document the morphological diversity that existed among stem mysticetes during the Oligocene. The skull and dentary of *Aetiocetus weltoni* preserve a number of features that underline the transitional nature of aetiocetids between dorudontine archaeocetes and crown mysticetes. The possession of an adult dentition in *A. weltoni* is seen as retention of an ancestral condition. The lateral palatal foramina on the palate of *A. weltoni* are interpreted as bony correlates for the presence of baleen. This heralds the major macroevolutionary shift in mysticetes from pierce feeding to bulk feeding using baleen. Concomitant with this, aetiocetids exhibit an early stage in development of an expanded oral cavity, another evolutionary novelty associated with bulk feeding.

Phylogenetic analysis confirms the monophyly of Aetiocetidae and recognizes *Morawanocetus* as the earliest diverging member of this clade. Species of *Aetiocetus* and *Chonecetus* share a more recent common ancestry. The speciose genus *Aetiocetus* appears to be monophyletic and its members document a limited range of morphological diversity including a trend toward polydonty.

Aetiocetids emerge as the most morphologically and taxonomically diverse clade of toothed mysticetes and are phylogenetically positioned between the southern hemisphere stem toothed mysticetes (*Janjucetus* and *Mammalodon*) and the crownward edentulous mysticetes.

ACKNOWLEDGEMENTS

We thank L. G. Barnes (LACM), Pat Holyroyd (UCMP) and H. Sawamura (AMP) for allowing us to study specimens under their care. The late Robert L. Clark skillfully prepared the holotype skull and dentaires of *Aetiocetus weltoni*. Glenn Daleo, formerly of San Diego Children's Hospital, provided CT imaging of UCMP 122900. Illustrations were produced by Barbara Marrs, Tim Gunther, Kesler Randall and Ian Browne. Research was supported in part by NSF grant DEB-0212238 to T.A.D. and grant DEB 0212248 to A.B.

REFERENCES

Addicott W. 1976. Neogene molluscan stages of Oregon and Washington. In: Fritsche AE, Best HT Jr, Wornardt WW, eds. *The Neogene Symposium*. San Francisco, CA: Society of Economic Paleontologists and Mineralogists, 95–116.

Armentrout JM. 1981. Correlation and ages of Cenozoic stratigraphic units in Oregon and Washington. *Geological Society of America Special Paper* **184:** 137–148.

Barnes LG, Kimura M, Furusawa H, Sawamura H. 1995. Classification and distribution of Oligocene Aetiocetidae (Mammalia; Cetacea; Mysticeti) from western North America and Japan. *Island Arc* **3:** 392–431.

Berta A, McGowen M, Gatesy J, Demere T. 2006. Mysticete phylogeny: the role of stem taxa and character evolution in the transition to modern mysticetes. *Journal of Vertebrate Paleontology* **26**: (Suppl. 3)**:** 42A.

Bouetel V, de Muizon C. 2006. The anatomy and relationships of *Piscobalaena nana* (Cetacea, Mysticeti), a Cetotheriidae *s.s*. from the early Pliocene of Peru. *Geodiversitas* **28:** 319–395.

Deméré TA. 1986. The fossil whale, *Balaenoptera davidsonii* (Cope 1872), with a review of other Neogene species of *Balaenoptera* (Cetacea: Mysticeti). *Marine Mammal Science* **2:** 227–298.

Deméré TA, Berta A, McGowen MR. 2005. The taxonomic and evolutionary history of fossil and modern balaenopteroid mysticetes. *Journal of Mammalian Evolution* **12:** 99–143.

Deméré TA, McGowen MR, Berta A, Gatesy JG. 2008. Morphological and molecular evidence for a stepwise evolutionary transition from teeth to baleen in mysticete whales. *Systematic Biology* **57:** 15–37.

Emlong DR. 1966. A new archaic cetacean from the Oligocene of northwest Oregon. *Bulletin of the Museum of Natural History, University of Oregon* **3:** 1–51.

Fitzgerald EMG. 2006. A bizarre new toothed mysticete (Cetacea) from Australia and the early evolution of baleen whales. *Proceedings of the Royal Society B: Biological Sciences* **273:** 2955–2963.

Fordyce RE. 1981. Systematics of the odontocete whale *Agorophius pygmaeus* and the Family Agorophiidae (Mammalia: Cetacea). *Journal of Paleontology* **55:** 1028–1045.

Fordyce RE. 1994. *Waipatia maerewhenua*, new genus and new species (Waipatiidae, new family), an archaic late Oligocene dolphin (Cetacea: Odontoceti: Plantanistoidea) from New Zealand. *Proceedings of the San Diego Society of Natural History* **29:** 147–176.

Fordyce RE. 2002. *Simocetus rayi* (Odontoceti: Simocetidae, New Family): a bizarre new archaic Oligocene dolphin from the eastern North Pacific. *Smithsonian Contributions to Paleobiology* **93:** 185–222.

Fordyce RE. 2003. Early crown-group Cetacea in the Southern Ocean: the toothed archaic mysticete Llanocetus. *Journal of Vertebrate Paleontology* **23** (Suppl. 3)**:** 50A.

Fordyce RE, Muizon C de. 2001. Evolutionary history of cetaceans: a review. In: Mazin J-M, de Buffrenil V, eds. *Secondary adaptations of tetrapods to life in water*. Munchen: Verlag Dr. Friedrich Pfeil, 169–233.

Geisler J, Sanders AE. 2003. Morphological evidence for the phylogeny of the Cetacea. *Journal of Mammalian Evolution* **10:** 23–129.

Harrison and Eaton (firm). 1920. Report on investigation of oil and gas possibilities of western Oregon. *Oregon Bureau of Mines and Geology, Mineral Resources. Oregon* **3:** 3–37.

Ichishima H. 2005. Notes on the phyletic relationships of the Aetiocetidae and the feeding ecology of toothed mysticetes. *Bulletin of Ashoro Museum of Paleontology* **3:** 111–117.

Ishikawa H, Amasaki H. 1995. Development and physiological degradation of tooth buds and development of rudiment of baleen plate in southern minke whale, *Balaenoptera acutorostrata*. *Journal of Veterinary Medical Science* **57:** 665–670.

Ishikawa H, Amasaki H, Dohguchi H, Furuya A, Suzuki K. 1999. Immunohistological distributions of fibronectin, tenascin, type I, III and IV collagens, and laminin during tooth development and degeneration in fetuses of minke whale, *Balaenoptera acutorostrata*. *Journal of Veterinary Medical Science* **61:** 227–232.

Karlsen K. 1962. Development of tooth germs and adjacent structures in the whalebone whale (*Balaenoptera physalus* (L.)). *Hvalrådets Skrifter* **45:** 5–56.

Kellogg R. 1923. Descriptions of two squalodonts recently discovered in the Calvert Cliffs, Maryland; and notes on the sharktoothed cetaceans. *Proceedings of the United States National Museum* **62:** 1–69.

Kellogg R. 1928. The history of whales – their adaptation to life in the water (concluded). *Quarterly Review of Biology* **3:** 174–208.

Kellogg R. 1936. A review of the Archaeoceti. *Carnegie Institute of Washington Special Publication* **482:** 1–366.

Kellogg R. 1969. Cetothere skeletons from the Miocene Choptank Formation of Maryland and Virginia. *United States National Museum Bulletin* **294:** 1–40.

Kimura M, Barnes LG, Furusawa H. 1992. Classification and distribution of Oligocene Aetiocetidae (Mammalia, Mysticeti) from western North America and Japan. *Abstracts, 29th International Geological Congress, Kyoto, Japan* **2:** 348.

Kleinpell RM. 1938. *Miocene stratigraphy of California*. Tulsa, OK: American Association of Petroleum Geologists.

Lambertsen R, Ulrich N, Straley J. 1995. Frontomandibular stay of Balaenopteridae: a mechanism for momentum recapture during feeding. *Journal of Mammalogy* **76:** 877–899.

Lambertsen RH. 1983. Internal mechanism of rorqual feeding. *Journal of Mammalogy* **64:** 76–88.

Luo Z, Gingerich PD. 1999. Terrestrial Mesonychia to aquatic Cetacea: transformation of the basicranium and evolution of hearing in whales. *University of Michigan Papers on Paleontology* **31:** 1–98.

McLeod SA, Whitmore FC, Barnes LG. 1993. Evolutionary relationships and classification. In: Burns JJ, Montague JJ, Cowles CJ, eds. *The bowhead whale*. Lawrence, KS: The Society for Marine Mammalogy, 45–70.

Messenger SL, McGuire JA. 1998. Morphology, molecules, and the phylogenetics of cetaceans. *Systematic Biology* **47:** 90–124.

Miller GS. 1923. The telescoping of the cetacean skull. *Smithsonian Miscellaneous Collections* **75:** 1–71.

Mitchell ED. 1989. A new cetacean from the late Eocene Meseta Formation, Seymour island, Antarctic Peninsula. *Canadian Journal of Fisheries and Aquatic Sciences* **46:** 2219–2235.

Muizon C de. 1984. Les Vertebres de al Formation Pisco (Perou). Deuxieme partie: Les Odontocetes (Cetacea, Mammalia) du Pliocene inferieur de Sud-Sacaco. *Travaux de Institut Français d'Études Andines* **27:** 1–188.

Muizon C de. 1991. A new Ziphiidae (Cetacea) from the early Miocene of Washington State (USA) and phylogenetic analysis of the major groups of odontocetes. *Bulletin du Muséum National d'Historie Naturelle, Section C 4ème série* **12:** 279–326.

Oelschlager HA. 1986. Comparative morphology and evolution of the otic region in toothed whales (Cetacea, Mammalia). *American Journal of Anatomy* **177:** 353–368.

Pivorunas A. 1977. The fibrocartilage skeleton and related structures of the ventral pouch of balaenopterid whales. *Journal of Morphology* **151:** 299–314.

Pivorunas A. 1979. The feeding mechanisms of baleen whales. *American Scientist* **67:** 432–440.

Pledge NS. 2005. A new species of early Oligocene cetacean from Port Willunga, South Australia. *Memoirs of the Queensland Museum* **51:** 123–133.

Prothero DR, Bitboul CZ, Moore GW, Niem AR. 2001. Magnetic stratigraphy and tectonic rotation of the Oligocene Alsea, Yaquina, and Nye formations, Lincoln County, Oregon. In: Prothero DR, ed. *Magnetic stratigraphy of the Pacific coast Cenozoic*. Pacific Section SEPM (Society for Sedimentary Geology) Book, vol. 91, 184–194.

Rau WW. 1981. Pacific Northwest Tertiary benthic foraminiferal biostratigraphic framework – An overview. *Geological Society of America Special Paper* **184:** 67–84.

Ridewood WG. 1923. Observations on the skull in foetal specimens of whales of the genera *Megaptera* and *Balaenoptera*. *Philosophical Transactions of the Royal Society of London, Series B* **211:** 209–272.

Russell LS. 1968. A new cetacean from the Oligocene Sooke Formation of Vancouver Island, British Columbia. *Canadian Journal of Earth Sciences* **5:** 929–933.

Sanders AE, Barnes LG. 2002. Paleontology of the late Oligocene Ashley and Chandler Bridge Formations of South Carolina, 3: Eomysticetidae, a new family of primitive mysticetes. *Smithsonian Contributions to Paleobiology* **93:** 313–356.

Sawamura H, Ichishima H, Ito H, Ishikawa H. 2006. Features implying the beginning of baleen growth in aetiocetids. *Journal of Vertebrate Paleontology* **26** (Suppl. 3)**:** 120A

Schulte HW. 1916. The sei whale (*Balaenoptera borealis* Lesson). Anatomy of the foetus of *Balaenoptera borealis*. Monographs of the Pacific Cetacea. *Memoirs of the American Museum of Natural History* **1:** 389–502.

Snaveley PD Jr, McLeod NS, Wagner HC, Rau WW. 1976. Geologic map of the Yaquina and Toledo quadrangles, Lincoln County, Oregon. *U.S.G.S. Miscellaneous Investigations Series Map*, I-867.

Swofford DL. 2001. *PAUP*' Phylogenetic analysis using parsimony (* and other methods)*. Version 4.0b8. Sunderland, MA: Sinauer Associates.

Uhen MD. 1999. New species of protocetid archaeocete whale, *Eocetus wardii* (Mammalia, Cetacea), from the middle Eocene of North Carolina. *Journal of Paleontology* **73:** 512–528.

Uhen MD. 2004. Form, function, and anatomy of *Dorudon atrox* (Mammalia: Cetacea): an archaeocete from the middle to late Eocene of Egypt. *University of Michigan Papers on Paleontology* **34:** 1–222.

Van Valen L. 1968. Monophyly or diphyly in the origin of whales. *Evolution* **22:** 37–41.

Walmsley R. 1938. Some observations on the vascular system of a female fetal finback. Carnegie Institution of Washington, Monograph Series 496. *Contributions to Embryology* **27:** 109–178.

APPENDIX 1

Characters and character states for Aetiocetids and related taxa

1. Rostrum, transverse width at midpoint relative to condylobasal length (Uhen, 1999). 0 = narrow (15–22%), 1 = very narrow (5–12%), 2 = broad (24–31%), 3 = very broad (> 31%).

The primitive condition of a narrow rostrum occurs in archaeocetes (e.g. *Dorudon* and *Zygorhiza*), the stem odontocete *Agorophius* and the stem edentulous mysticete *Eomysticetus*. A very narrow rostrum represents derived condition 1 and is seen in some odontocetes (e.g. *Tasmacetus*). *Mammalodon*, *Janjucetus* and all aetiocetids are characterized by having a broad rostrum (derived condition 2). Certain balaenopterids are coded as having very broad rostra (derived condition 3). Crown balaenids show a reversal to a very narrow rostrum.

2. Frontal, supraorbital process (modified from Miller, 1923). 0 = broad anteroposteriorly and short transversely, 1 = moderately broad anteroposteriorly and moderately elongate transversely, 2 = very narrow anteroposteriorly and very elongate transversely.

Archaeocete cetaceans such as *Dorudon* and *Zygorhiza*, as well as aetiocetids, possess an anteroposteriorly broad, but transversely short supraorbital process of the frontal; the primitive condition. In derived condition 1 the anteroposterior diameter of the frontals is reduced, while the transverse diameter is increased. This is the condition seen in *Eomysticetus* and balaenopteroids. Pliocene through Holocene balaenids possess derived condition 2, a frontal that is narrow anteriorposteriorly, but elongated transversely.

3. Frontal, posteromedial corner. 0 = well exposed, 1 = short overlap by maxilla, 2 = broadly overlapped by maxilla.

The primitive condition of a broadly exposed frontal occurs in *Dorudon* and *Zygorhiza*. Derived condition 1, posteromedial corner of frontal overlapped by maxilla, characterizes *Janjucetus*, *Mammalodon*, aetiocetids and edentulous mysticetes. Derived condition 2, broad overlap of frontal by maxilla, distinguishes odontocetes.

4. Parietal–frontal suture, anterior extension. 0 = none, 1 = lobate, 2 = triangular.

The primitive condition of a nearly transverse parietal–frontal (coronal) suture occurs in *Dorudon*, *Zygorhiza* and all odontocetes. Two derived conditions are identified. A lobate anterior extension of the parietal frontal contact occurs in species of *Aetiocetus* (derived condition 1). A triangular anterior extension characterizes *Chonecetus* (derived condition 2). The condition in *Morawanocetus* and *Mammalodon* is currently unknown.

5. Nasals, width relative to length (Deméré *et al.*, 2005). 0 = slender (15–25%), 1 = broad (26–45%), 2 = very broad (46–70%), 3 = extremely broad (> 71%).

In *Zygorhiza* the width of the nasals represents only 18% of the length. In *Mammalodon*, *Janjucetus* and

aetiocetids (except *A. polydentatus*) the nasals are broader and nasal width relative to length is as follows: *Aetiocetus cotylalveus* (31%), *A. weltoni* (31%), *Chonecetus goedertorum* (30%). As noted by Barnes *et al.* (1995), *Aetiocetus polydentatus* is the only aetiocetid with very broad nasals (47%), identified as derived state 2. The basal odontocete *Agorophius* exhibits extremely broad nasals (derived state 3) approximately 50% as estimated from the line drawings in Fordyce (1981).

6. Frontal, orbital rim (Barnes *et al.*, 1995). 0 = straight, 1 = slightly concave, 2 = deeply concave.

The primitive condition of a straight orbital rim (in dorsal aspect) occurs in *Zygorhiza*, *Dorudon* and odontocetes. An intermediate condition, derived condition 1, in which the orbital rim is slightly concave, occurs in *Mammalodon*, *Janjucetus*, *Aetiocetus tomitai*, *A. polydentatus*, *Morawanocetus*, *Chonocetus*, *Eomysticetus* and some other edentulous mysticetes. Derived condition 2, a deeply concave orbital rim, is a synapomorphy for *A. cotylalveus* and *A. weltoni*. Some crown mysticetes (e.g. *Balaenoptera acutorostrata*) show a reversal to the primitive condition.

7. Ascending process of maxilla, posterior termination (Deméré *et al.*, 2005). 0 = anterior half of supraorbital process of frontal, 1 = anterior border of supraorbital process of frontal, 2 = posterior half of supraorbital process of frontal, 3 = Posterior to temporal fossa.

The primitive condition, where the ascending process of the maxilla terminates within the anterior half of the supraorbital process of the frontal, characterizes *Zygorhiza*, *Dorudon*, *Janjucetus*, *Mammalodon* and all aetiocetids (except *A. weltoni*). In derived condition 1 seen in *Eomysticetus*, the posteriormost edge of the ascending process of the maxilla extends only to the anterior border of the supraorbital process of the frontal. In *Aetiocetus weltoni*, the posteriormost edge of the ascending process of the maxilla terminates within the posterior half of the supraorbital process of the frontal, derived condition 2. This is also the condition in *Agorophius*. In *Tasmacetus* the posteriormost edge of the ascending process of the maxilla extends posterior to the temporal fossa, derived condition 3.

8. Intertemporal region. 0 = narrow, 1 = broad.

In the primitive condition, seen in *Dorudon*, *Zygorhiza*, *Aetiocetus polydentatus*, *A. weltoni*, *Mammalodon* and *Eomysticetus*, the intertemporal region is narrow (< 70% width across occipital condyles). All other aetiocetids, *Janjucetus* and later diverging edentulous mysticetes show the derived condition of a broad intertemporal region (> 80% width across occipital condyles).

9. Sagittal crest. 0 = present, 1 = reduced, 2 = absent.

The presence of a well-developed sagittal crest is the primitive condition seen in *Dorudon*, *Zygorhiza*, *Janjucetus* and *Eomysticetus*. Derived condition 1, reduction of the sagittal crest, occurs in *Mammalodon*, *Aetiocetus weltoni* and *A. polydentatus*. In all other described aetiocetids, as well as edentulous mysticetes a sagittal crest is absent.

10. Squamosal, zygomatic process thickness. 0 = uniform thickness entire length, 1 = expanded near anterior margin and at the posterior end but narrow in the middle.

In the primitive condition, seen in outgroup taxa and *Janjucetus*, *Chonecetus* and *Eomysticetus*, the zygomatic process is of uniform width. The derived condition, in which the zygomatic process is thin in the middle and expanded anteriorly and posteriorly, represents an aetiocetid synapomorphy. Edentulous mysticetes display a reversal to the primitive condition.

11. Squamosal, zygomatic process length. 0 = does not contact postorbital process of frontal, 1 = contacts postorbital process of frontal.

In the primitive condition, seen in *Dorudon*, *Zygorhiza*, *Agorophius* and *Eomysticetus*, the zygomatic process of the squamosal does not contact the postorbital process of the frontal. The derived condition, in which the zygomatic process contacts the postorbital process of the frontal, characterizes *Tasmacetus*, *Janjucetus*, species of *Aetiocetus*, *Morawanocetus* and modern mysticetes; this distribution indicates independent derivation among odontocetes and aetiocetids.

12. Lacrimal, external exposure. 0 = exposed laterally, 1 = exposed dorsally.

In the primitive condition, seen in archaeocetes, odontocetes and *Janjucetus* the lacrimal is well exposed laterally between the frontal and maxilla. In crown mysticete taxa the lacrimal retains a lateral exposure, but is tightly sandwiched between the frontal and antorbital process of the maxilla. Aetiocetids display the derived condition in which the lacrimal is a broadly oval element exposed dorsally.

13. Palatal window, exposing vomer (Deméré *et al.*, 2008). 0 = absent, 1 = present, delimited entirely by maxilla, 2 = present, delimited by maxilla and premaxilla.

In the primitive condition, seen in *Zygorhiza* and *Dorudon*, the vomer is hidden from view on the palate by the maxilla. In *Janjucetus* the vomer is exposed in a narrow palatal window formed by the maxilla (derived condition 1). This appears also to be the condition in *Tasmacetus*. In all aetiocetids with preserved palates the vomer is exposed in a narrow palatal window formed by bifurcation of the maxilla

and premaxilla (derived condition 2), a synapomorphy for the group. The absence of a palatal window exposing the vomer in crown mysticetes appears to represent retention of the primitive condition.

14. Palatine, posterior margin with notch. 0 = absent 1 = present.

In the primitive condition, seen in *Dorudon*, *Zygorhiza*, *Agorophius*, *Tasmacetus*, *Janjucetus* and crown mysticetes, the posterior margin of the palatine has a smooth margin. The derived condition, in which the posterior margin of the palatine has a rectangular notch, occurs in aetiocetids and represents a synapomorphy for the group.

15. Palatines, posterior termination. (Deméré *et al.*, 2005). 0 = extend to internal nares, 1 = extend to slightly overlap the pterygoids, 2 = long overlap of pterygoids nearly reaching pterygoid fossa.

In the primitive condition, seen in *Dorudon*, *Zygorhiza*, *Janjucetus*, aetiocetids and odontocetes, the palatines are long and narrow posteriorly. The derived condition, in which the palatines have a short and broad extension that overlaps the pterygoid, occurs in modern mysticetes.

16. Lateral palatine foramina (modified from Geisler & Sanders, 2003). 0 = absent, 1 = present.

In the primitive condition, seen in *Dorudon*, *Zygorhiza*, odontocetes and *Janjucetus*, the lateral portion of the maxilla on the palate lacks nutrient foramina. The derived condition, in which foramina and associated short sulci are positioned along the lateral portion of the maxilla, occurs in all edentulous mysticetes. Although more diminutive than in crown mysticetes, the tiny foramina and sulci found alongside and medial to the alveoli (see text) in aetiocetids are considered homologous.

17. Squamosal fossa (Barnes *et al.*, 1995). 0 = single, continuous fossa, 1 = second fossa.

In the primitive condition, seen in outgroup taxa, *Mammalodon* and *Morawanocetus*, a single, shallow, continuous squamosal fossa is developed. The derived condition, in which a second smaller fossa is developed posterior to the squamosal fossa creating a 'stepped' profile, occurs in *Janjucetus*, *Chonecetus* and species of *Aetiocetus*.

18. Basicranial width. 0 = narrow, 1 = wide.

The relative width of the anterior and posterior borders of the basioccipital varies among mysticetes. In species of *Aetiocetus* and *Chonocetus* the two measurements are subequal (primitive condition). In the derived condition, seen in *Morawanocetus* and *Janjucetus*, the posterior measurement is distinctly larger (> 1.5 times) than the anterior measurement. The derived condition is also seen in odontocetes, a distribution suggesting independent derivation among odontocetes and aetiocetids.

19. Posterior sinus. 0 = poorly developed or absent, 1 = present.

In the primitive condition, seen in *Dorudon*, *Zygorhiza*, *Eomysticetus* and modern mysticetes, the posterior sinus is poorly developed or absent. In aetiocetids, the posterior sinus is well formed. The derived condition is also seen in certain odontocetes (e.g. *Tasmacetus*), a distribution suggesting independent derivation among odontocetes and aetiocetids.

20. Posterior teeth, root condition. 0 = two rooted with fused roots, 1 = double rooted, 2 = single rooted.

In the primitive condition, seen in *Dorudon* and *Zygorhiza*, P4 and M1 are two-rooted with the posterior root developed from fusion of two separate roots. In *Agorophius*, *Janjucetus* and *Morawanocetus* the posterior teeth are double rooted, derived condition 1. In *Mammalodon* the posterior upper teeth appear to have single fused roots. However, in the lower dentition the posterior teeth are clearly double rooted. Because of this, *Mammalodon* is here considered to possess condition 1. Species of *Aetiocetus* and *Chonecetus* (based on alveoli only) are characterized by upper and lower single rooted teeth, derived condition 2.

21. Number of teeth (Deméré *et al.*, 2008). 0 = 10/11, 1 = 11/12, 2 = 13-14/14-14.

In the primitive condition, seen in *Dorudon*, *Zygorhiza*, *Agorophius* and *Janjucetus*, the dental formula is 10/11. In *Mammalodon* and aetiocetids (except for *A. polydentatus*) the dental formula is 11/12, derived condition 1. *Aetiocetus polydentatus* displays derived condition 2, a high tooth count (polydonty), 13-14/14-14. The high tooth count of *Tasmacetus* is also scored as derived condition 2 and suggests independent evolution of polydonty in both odontocetes and mysticetes.

22. Postcanine tooth enamel (Deméré *et al.*, 2008). 0 = delicate vertical enamel ridges on lingual surface only, 1 = very heavy vertical enamel ridges on lingual and labial surfaces, 2 = enamel ridges poorly developed or absent.

Zygorhiza has stronger enamel ridges on the lingual surfaces of P2-4 than on the labial sides of these teeth, while M1-2 have essentially smooth enamel surfaces on both the lingual and the labial sides (Kellogg, 1936). Species of *Aetiocetus* have delicate vertical enamel ridges on the lingual sides of the cheektooth crown and smooth enamel on the labial sides (primitive condition). *Janjucetus*, *Mammalodon* and *Morawanocetus* are characterized by derived condition 1, heavy enamel ridges on both the labial and the lingual sides of the cheek tooth crowns. Derived

condition 2, in which striated enamel is poorly developed or absent, characterizes *Tasmacetus*.

23. Posterior upper postcanine teeth (Deméré *et al.*, 2008). 0 = five or more, large and well-developed anterior and posterior denticles, 1 = three or fewer, small and simple anterior and posterior denticles.

Dorudon, *Zygorhiza*, *Agorophius*, *Janjucetus* and *Morawanocetus* show an increase in number and complexity of accessory denticles on the posterior postcanine teeth; the primitive condition. Species of *Aetiocetus* have fewer, simpler denticles on the postcanine teeth; derived condition 1. The condition in *Mammalodon* is equivocal because of heavy apical crown wear in the holotype. Because of this *Mammalodon* is coded as unknown. *Chonecetus* is also scored as unknown, because of the lack of preserved dentitions for this genus.

24. Upper teeth, diastemata (Deméré *et al.*, 2008). 0 = teeth with wide diastemata, 1 = teeth closely appressed or with nearly equally narrow diastemata.

The upper dentition of *Zygorhiza* and *Dorudon* consists of anterior teeth (I1-3, C, P1-2) with relatively wide diastemata and posterior teeth (P2-4, M1-2) more closely appressed. In species of *Aetiocetus*, the anterior teeth in the upper dentition also have wide diastemata, while the more posterior teeth have narrow diastemata. The derived condition, in which the alveoli of the upper dentition are of nearly equally narrow width or are closely appressed, occurs in *Chonecetus* and *Janjucetus*, and *Mammalodon*, respectively. The condition in *Morawanocetus* is unknown.

25. Dentary, outline in dorsal aspect (modified from Miller, 1923; Deméré, 1986). 0 = laterally concave, 1 = straight, 2 = laterally convex.

In the primitive condition, seen in archaeocetes, odontocetes and possibly *Janjucetus* (see Fitzgerald, 2006), the dentary is laterally concave in dorsal aspect. Two derived conditions are identified in mysticetes. Derived condition 1, a relatively straight dentary in dorsal aspect (e.g. the straight length of the dentary does not exceed 97% of the curved length), occurs in aetiocetids and *Eomysticetus*, as well as *Eschrichtius*. In other crown mysticetes (e.g. balaenopterids and balaenids) the dentary is laterally convex; derived condition 2 (Deméré *et al.*, 2005).

26. Mandibular symphysis (Geisler & Sanders, 2003; Fitzgerald, 2006). 0 = sutured, but unfused, 1 = unsutured, with shallow elongate fossa, 2 = unsutured, with long groove.

Archaeocetes and odontocetes have a symphysis that is sutured, but typically unfused; the primitive condition. All mysticetes have a symphysis that is unfused and unsutured. Instead, the symphysis is held together by soft tissue (fibrocartilage; Pivorunas, 1977). Two derived conditions are identified in mysticetes. Derived condition 1, symphysis with a shallow, elongate fossa, is reported in *Janjucetus* and *Mammalodon* (see Fitzgerald, 2006). Derived condition 2, symphysis with a long groove and overlying narrow shelf, occurs in aetiocetids and all later diverging mysticetes.

27. Dentary, coronoid process. 0 = broad, with posterior margin nearly vertical and slightly overhanging, 1 = well developed, with concave posterior margin, 2 = reduced, 3 = finger-like or crest-like

In the primitive condition, seen in *Dorudon*, *Zygorhiza*, *Janjucetus* and *Mammalodon*, the coronoid process has a broad base and its posterior margin is generally straight. In aetiocetids the coronoid process is also well developed, but its posterior margin is concave; derived condition 1. A reduced coronoid process characterizes odontocetes and modern mysticetes, which possess coronoid processes that are either finger-like or crest-like; derived condition 2.

28. Nasal, posterior margin (modified from Geisler & Sanders, 2003). 0 = located at or just in front of anterior edge of supraorbital process of frontal, 1 = located in line with anterior half of supraorbital process of frontal, 2 = located in line with posterior half of supraorbital process of frontal, 3 = located posterior to temporal fossa.

Cranial telescoping plays a prominent role in cetacean evolution and involves the relocation of the external nares from an anterior position at the front of the rostrum to a progressively more posterior position above or behind the orbits. One measure of the degree of telescoping is the location of the nasal-frontal suture relative to the supraorbital process of the frontal. In the primitive condition the posterior border of the nasal lies at or just anterior to the supraorbital process of the frontal. This condition occurs in archaeocetes, *Janjucetus*, *Mammalodon* and *Morawanocetus*. In derived state 1 the posteriormost edge of the nasal extends to a level above the centre of the orbit on the anterior border of the supraorbital process of the frontal. This is the condition in some crown mysticetes. In derived state 2 the posteriormost edge of the nasal extends to the posterior half of the supraorbital process of the frontal. This is the condition in *Aetiocetus* spp., *Chonecetus* and *Eomysticetus*, as well as in the basal odontocete *Agorophius*. In derived state 3, seen in *Tasmacetus*, the posteriormost edge of nasal extends to the posterior half of the temporal fossa.

29. Maxilla, descending process (modified from McLeod, Whitmore & Barnes, 1993). 0 = present, with teeth, 1 = present, as edentulous infraorbital plate, 2 = absent.

The posterior portion of the maxilla is divided in cetaceans into ascending and descending processes. In mysticetes the descending process becomes transversely expanded to form the infraorbital plate. Beginning with Miller (1923) the presence of an infraorbital plate of the maxilla has been considered a diagnostic feature of mysticetes. In archaeocetes the descending process houses the M1-3 toothrow and is not developed as an edentulous infraorbital plate (primitive condition). In aetiocetids and other toothed mysticetes, as well as all edentulous mysticetes, the descending process is expanded into an infraorbital plate (derived condition 1). Interestingly, even in the toothed aetiocetids the infraorbital plate is edentulous. In odontocetes there is no descending process of the maxilla (derived condition 2).

30. Supraoccipital shield, orientation. 0 = vertically orientated, 1 = anteriorly sloped dorsal portion.

In the primitive condition, seen in archaeocetes, *Janjucetus* and certain odontocetes (e.g. *Tasmacetus*), the supraoccipital shield is orientated vertically to overhanging. The derived condition, an anterodorsally sloped supraoccipital shield, occurs in all other toothed and edentulous mysticetes. The presence of an anterodorsally sloped supraoccipital shield in the outgroup taxon *Agorophius* suggests independent evolution of this feature.

31. Frontal, supraorbital process. 0 = at level of vertex, 1 = gradually sloping or abruptly depressed below vertex.

In the primitive condition, seen in archaeocetes, *Janjucetus*, *Mammalodon*, aetiocetids, *Eomysticetus* and odontocetes, the supraorbital process of the frontal is positioned at the level of the cranial vertex. In the derived condition, seen in later diverging mysticetes, the supraorbital process lies below the vertex. Variation of the derived state includes a gradually sloping supraorbital process (e.g. most 'cetotheres' and crown balaenids) and an abruptly depressed supraorbital process (e.g. balaenopteroids).

32. Teeth. 0 = anterior and postcanine teeth strongly heterodont, 1 = anterior and postcanine teeth moderately heterodont, 2 = anterior and postcanine teeth weakly heterodont, 3 = teeth homodont.

In the primitive condition, seen in archaeocetes and *Agorophius*, the postcanine teeth are strongly heterodont (i.e. relatively large denticles). In *Mammalodon*, *Janjucetus* and *Morawanocetus* postcanine teeth are moderately heterodont (i.e. distinct, but small denticles); derived condition 1. In species of *Aetiocetus* the postcanine teeth have very small, delicate denticles; derived condition 2. In *Tasmacetus* the dentition is distinctly homodont; derived condition 3.

33. Squamosal, subtemporal crest (Fordyce, 2002). 0 = absent, 1 = present.

In the primitive condition, seen in *Dorudon*, *Tasmacetus*, *Mammalodon*, *Janjucetus*, *Eomysticetus* and modern mysticetes, the posterior border of the temporal fossa is evenly concave and there is no subtemporal crest. The derived condition, a distinct subtemporal crest extending into the temporal fossa, occurs in *Zygorhiza*, stem odontocetes (e.g. *Agorophius*) and aetiocetids.

34. Lambdoidal crests. 0 = flush with temporal wall, 1 = overhanging temporal wall.

In the primitive condition, seen in archaeocetes, *Tasmacetus* and aetiocetids (except *A. polydentatus*), the lambdoidal crests are low and subequal to the temporal wall. The derived condition, lambdoidal crests that overhang the temporal wall, occurs in *Agorophius*, *Mammalodon*, *Janjucetus*, *Aetiocetus polydentatus* and *Eomysticetus*. The condition in crown mysticetes is polymorphic.

35. External narial fossa, position (Deméré *et al.*, 2005). 0 = located between midpoint of rostrum and antorbital notch, 1 = located inline with or just posterior to antorbital notch, 2 = located well posterior to antorbital notch.

The position of the external narial fossa on the rostrum tracks the posterior migration of the blowhole in cetacean evolution. In the primitive condition, seen in *Zygorhiza*, *Dorudon*, *Mammalodon*, aetiocetids and *Eomysticetus*, the narial fossa is anteriorly located between the midpoint of the rostrum and the antorbital notch. Two derived conditions are recognized. Derived condition 1, narial fossa positioned inline with or just posterior to the antorbital notch, occurs in *Agorophius*. Derived condition 2, narial fossa positioned well posterior to the antorbital notch, occurs in *Tasmacetus* and other extant odontocetes. Crown mysticetes are polymorphic for this character and display both the primitive condition (e.g. balaenids and neobalaenids) and derived condition 1 (e.g. balaenopteroids).

36. Jugal, contact with squamosal. 0 = broad overlap, 1 = short overlap, 2 = no overlap, ligamentous.

Primitively, the contact between the jugal and zygomatic process of the squamosal is broadly overlapping. The primitive condition occurs in archaeocetes (e.g. *Dorudon* and *Zygorhiza*). In aetiocetids the zygomatic process still overlaps the jugal, but the degree of overlap is very reduced (derived state 1). In derived state 2 the jugal is not overlapped by the

zygomatic process. This is the condition in *Tasmacetus*, *Eomysticetus* and modern mysticetes.

37. Ascending process of maxilla, position of posterior end (Bouetel & de Muizon, 2006). 0 = located anterior to posterior margin of nasal; 1 = located approximately inline with or slightly posterior to posterior margin of nasal.

In the primitive condition, seen in *Dorudon*, *Janjucetus*, *Aetiocetus tomitai* and *Chonecetus*, the posterior termination of the ascending process of the maxilla lies anterior to the posterior termination of the nasal. The derived condition, ascending process of maxilla terminating inline with or behind the nasal, occurs in the majority of aetiocetids and crown mysticetes (except balaenids).

38. Premaxilla, position of posterior end (Bouetel & de Muizon, 2006). 0 = located anterior to posterior extremity of maxilla; 1 = located inline with posterior extremity of maxilla; 2 = located posterior to posterior extremity of maxilla.

The relative position of the posterior termini of the premaxilla and maxilla varies among cetaceans. In the primitive condition, seen in *Zygorhiza*, *Dorudon*, *Janjucetus* and *Mammalodon*, the premaxilla terminates anterior to the maxilla. Two derived conditions are recognized. In derived condition 1, the premaxilla and maxilla terminate at approximately the same level. This is the condition in *Morawanocetus*, *Aetiocetus weltoni*, *A. cotylalveus* and crown mysticetes. In derived state 2, the premaxilla terminates behind the posterior extremity of the maxilla. This is the condition in *Eomysticetus*, *Aetiocetus tomitai*, *A. polydentatus* and *Chonecetus*.

39. Maxilla, antorbital process (modified from Geisler & Sanders, 2003). 0 = no groove on anterolateral face; 1 = oblique groove on anterolateral face present, but low; 2 = oblique groove on anterolateral face present and well developed.

The anterolateral face of the antorbital process of the maxilla merges smoothly with the rostral portion of the maxilla in archaeocetes and odontocetes (primitive condition). In mysticetes the two regions are distinctly separated and the anterolateral face of the antorbital process is more steeply orientated than the rostral portion. In mysticetes this area is crossed obliquely (posteroventrolateral to anterodorsomedial) by a distinct groove for the facial nerve. Development of this groove is variable, being weakly developed in *Chonecetus* and modern mysticetes (derived condition1) and strongly developed in *Janjucetus*, *Mammalodon* and species of *Aetiocetus* (derived condition 2).

40. Rostrum, width at antorbital notch (modified from Geisler & Sanders, 2003). 0 = 130–165% of occipital condyle width; 1 = > 170% of occipital condyle width.

In the primitive condition, seen in outgroup taxa (except *Agorophius*) and *Chonecetus*, the rostrum as measured at the antorbital notch is narrow. In the derived condition, seen in species of *Aetiocetus* and some crown mysticetes, the rostrum is expanded, a feature correlated with enlargement of the oral cavity. The narrow rostra of crown balaenids represents a reversal to the primitive condition.

41. Palate, shape (Messenger & McGuire, 1998). 0 = flat with no median keel, 1 = median keel dividing palate into right and left concave surfaces.

In the primitive condition, seen in outgroup taxa and toothed mysticetes, the palate is relatively flat. The derived condition, in which there is a well-developed median keel dividing the palate into right and left halves, occurs in edentulous mysticetes.

42. Mineralized teeth in adults (Geisler & Sanders, 2003). 0 = present, 1 = absent.

The presence of teeth is the primitive condition seen among diverse archaic toothed taxa including archaeocetes, stem mysticetes and stem odontocetes. The derived condition, in which adult mineralized teeth are absent, is a synapomorphy for all edentulous mysticetes. In several species of odontocetes (i.e. delphinapterines and ziphiids) a mineralized dentition has been secondarily lost in adult female individuals.

43. Frontal, temporal crest (Geisler & Sanders, 2003). 0 = does not extend far onto dorsal surface of supraorbital process of frontal, 1 = extends far onto dorsal surface of supraorbital process of frontal.

In the primitive condition, seen in outgroup taxa and toothed mysticetes, the temporal crest does not extend onto the dorsal surface of the supraorbital process of the frontal. The derived condition, in which the temporal crest extends far onto the supraorbital process of the frontal, characterizes all edentulous mysticetes and is correlated with the anterior expansion of the temporalis musculature.

44. Premaxilla–maxilla suture (Geisler & Sanders, 2003). 0 = fused dorsally along rostrum, 1 = unfused.

Rostral kinesis (i.e. loose articulations between premaxilla, maxilla and vomer) appears to be an important feature in bulk feeding. In the primitive condition, seen in outgroup taxa and toothed mysticetes, the premaxilla–maxilla suture is fused along the dorsal and ventral portions of the rostrum. The derived condition, in which the premaxilla–maxilla suture is unfused, occurs in edentulous mysticetes.

45. Maxilla, lateral margin (modified from McLeod *et al.*, 1993); 0 = thick, 1 = thin.

In the primitive condition, seen in outgroup taxa and the toothed mysticete *Janjucetus*, the lateral margin of the maxilla is thick. The derived condition, in which the lateral margin of the maxilla is thin, occurs in *Mammalodon*, aetiocetids and edentulous mysticetes.

46. Premaxilla, ascending process (modified from Miller, 1923). 0 = no contact with frontals, 1 = contacting the frontals, 2 = contacting frontals and forming robust ascending process.

In the primitive condition, seen in archaeocetes and stem odontocetes, the ascending process of the premaxilla does not contact the frontals. Derived condition 1, in which the premaxilla weakly contacts the frontals, occurs in *Janjucetus* and *Morawanocetu*s. Derived condition 2, in which the premaxilla contacts the frontals and forms a robust ascending process, occurs in aetiocetids (except *Morawanocetus*). Crown mysticetes are polymorphic for this character.